

## RESEARCH ARTICLE

# Spalt-like 4 promotes posterior neural fates via repression of *pou5f3* family members in *Xenopus*

John J. Young\*, Rachel A. S. Kjolby, Nikki R. Kong, Stefanie D. Monica and Richard M. Harland†

## ABSTRACT

Amphibian neural development occurs as a two-step process: (1) induction specifies a neural fate in undifferentiated ectoderm; and (2) transformation induces posterior spinal cord and hindbrain. Signaling through the Fgf, retinoic acid (RA) and Wnt/β-catenin pathways is necessary and sufficient to induce posterior fates in the neural plate, yet a mechanistic understanding of the process is lacking. Here, we screened for factors enriched in posterior neural tissue and identify *spalt-like 4* (*sall4*), which is induced by Fgf. Knockdown of *Sall4* results in loss of spinal cord marker expression and increased expression of *pou5f3.2* (*oct25*), *pou5f3.3* (*oct60*) and *pou5f3.1* (*oct91*) (collectively, *pou5f3* genes), the closest *Xenopus* homologs of mammalian stem cell factor *Pou5f1* (*Oct4*). Overexpression of the *pou5f3* genes results in the loss of spinal cord identity and knockdown of *pou5f3* function restores spinal cord marker expression in *Sall4* morphants. Finally, knockdown of *Sall4* blocks the posteriorizing effects of Fgf and RA signaling in the neurectoderm. These results suggest that *Sall4*, activated by posteriorizing signals, represses the *pou5f3* genes to provide a permissive environment allowing for additional Wnt/Fgf/RA signals to posteriorize the neural plate.

**KEY WORDS:** Oct4, *Sall4*, *Xenopus*, Gene regulation, Neural patterning

## INTRODUCTION

Nieuwkoop and Eyal-Giladi suggested that development of the amphibian central nervous system arises by ‘activation and transformation’ (Nieuwkoop, 1952; Nieuwkoop et al., 1952a, 1952b; Eyal-Giladi, 1954) whereby neural tissue is induced as an anterior state by the organizer and then posteriorized by additional signals from the mesoderm to specify the anterior-posterior (A-P) pattern of the neural plate. Activation, or neural induction, requires bone morphogenetic protein (Bmp) antagonists, such as Noggin (Lamb et al., 1993), Chordin (Sasai et al., 1994) and Follistatin (Hemmati-Brivanlou et al., 1994), from the organizer to induce the neural fate (Khokha et al., 2005). Indeed, any manipulation that blocks Bmp signaling in ectoderm results in anterior neural fates (Hemmati-Brivanlou and Melton, 1994). Caudalization, or transformation, occurs via signaling by retinoic acid (RA) (Durston et al., 1989; Sive et al., 1990; Ruiz i Altaba and Jessell, 1991; Blumberg et al., 1997; Kolm et al., 1997), Fgf (Cox and Hemmati-Brivanlou, 1995; Kengaku and Okamoto, 1995; Lamb and Harland, 1995; Ribisi et al., 2000; Fletcher et al., 2006) and

Wnt/β-catenin (McGrew et al., 1995; Itoh and Sokol, 1997; Domingos et al., 2001; Erter et al., 2001; Kiecker and Niehrs, 2001). Despite the identification of these secreted factors as mediators of A-P neural patterning, the mechanism by which transduction of these signals results in the adoption of posterior fates remains poorly understood.

Given the interest in axial patterning, a few transcription factors that mediate A-P differentiation have been identified. The homeobox gene *gbx2* is a direct target of canonical Wnt signaling and primarily serves to localize the isthmus and induce neural crest (Simeone, 2000; Li et al., 2009). The *meis3* gene, which is required for hindbrain and neuronal differentiation, is directly activated by Wnt3a from the dorsal lateral marginal zone (Elkouby et al., 2010, 2012). The caudal homologs *Cdx1* and *Cdx4* are direct Wnt targets in the mouse (Prinos et al., 2001; Pilon et al., 2006, 2007) and have overlapping roles in posterior development of the three germ layers (Isaacs et al., 1998; Faas and Isaacs, 2009; van de Ven et al., 2011). In the neural plate of *Xenopus*, simultaneous knockdown of *Cdx1*, *Cdx2* and *Cdx4* is required to block adoption of the most posterior neural fates (Faas and Isaacs, 2009).

The Spalt-like (Sall) proteins are vertebrate homologs of the *Drosophila* protein Spalt. The four members of the Sall family of zinc-finger transcription factors in vertebrates contain an N-terminal C2HC zinc-finger domain followed by variable numbers of doublet and triplet C2H2 zinc-finger domains (Sweetman and Münsterberg, 2006; de Celis and Barrio, 2009). *Sall1* and *Sall4* function as either transcriptional repressors (Lauberth and Rauchman, 2006; Lauberth et al., 2007; Lu et al., 2009; Yang et al., 2012) or activators (Kiefer et al., 2002; Zhang et al., 2006; Yang et al., 2007; Lim et al., 2008). Mutations in human *SALL1* and *SALL4* cause the autosomal dominant Townes-Brocks and Okihiro syndromes, respectively, both characterized by limb and cognitive defects (Kohlhase et al., 1998, 2002). *Sall4* knockout mice fail to maintain a pluripotent inner cell mass (Sakaki-Yumoto et al., 2006); null embryos lack *Pou5f1* (*Oct4*) expression in the ICM, increase *Cdx2* expression and replace epiblast with trophectoderm (Wu et al., 2006; Zhang et al., 2006). Furthermore, knockdown of *Sall4* inhibits induction of induced pluripotent stem cells (iPSCs) (Tsubooka et al., 2009).

Previously, *sall2*, *sall3* and *sall4* were shown to be expressed during early *Xenopus* embryogenesis (Holleman et al., 1996; Onuma et al., 1999; Onai et al., 2004) and, with the exception of *sall2* (Onai et al., 2004), were expressed in posterior neural regions. Conditional knockouts of *Sall1*, *Sall2* and *Sall4* result in mouse embryos with neural tube closure defects (Böhm et al., 2008), revealing a role for these genes in neural differentiation or morphogenesis. Despite their expression in posterior neural regions of vertebrate embryos, a role for the Sall genes in caudalization has not been elucidated.

Here we describe the results of an expression screen designed to discover targets of canonical Wnt signaling that determine neural posteriorization in *Xenopus*. This screen identified *sall1* and *sall4* as targets in neuralized tissue. We show that *sall4* is required for

Department of Molecular & Cell Biology, University of California, Berkeley, CA 94720, USA.

\*Present address: Department of Genetics, Harvard Medical School, Boston, MA 02115, USA.

†Author for correspondence (harland@berkeley.edu)

Received 24 May 2013; Accepted 19 February 2014

caudalization and, importantly, spinal cord differentiation of neural tissue. Finally, we show that *sall4* represses the stem cell factor *pou5f3* to release cells from an undifferentiated state.

## RESULTS

### Screen to identify posterior neural patterning genes

We used the inducible  $\beta$ -catenin analog TVGR (TCF/LEF DNA-binding domain fused to both the VP-16 transactivation domain and growth hormone receptor) to mimic a posteriorizing Wnt signal (Darken and Wilson, 2001). Having confirmed that this treatment effectively activates Wnt signaling in response to DEX using ventral vegetal injections (supplementary material Fig. S1A), we tested the activity of TVGR in posteriorizing neural tissue using ectodermal explants treated at later stages. Animal caps overexpressing Noggin expressed the anterior neural marker *otx2* but not *epidermal keratin*, demonstrating that the explants had adopted a neural fate. By contrast, neuralized caps, which were injected with TVGR and induced with DEX, expressed the posterior markers *krox20* and *hoxb9*. Ethanol vehicle did activate the hindbrain marker *krox20*, but DEX was required to induce spinal cord fates as assayed by *hoxb9* expression (supplementary material Fig. S1B). Consistent with these results, activation of TVGR in neuralized animal caps induced convergent extension-like morphogenesis consistent with differentiation into spinal cord (Elul et al., 1997) (supplementary material Fig. S1C).

Next, we validated the use of activated TVGR in neuralized animal caps to enrich for transcriptional targets of Wnt signaling (supplementary material Fig. S2A). Treatment with the translational inhibitor cycloheximide (CHX) did not prevent activation of the direct target *meis3* (Elkouby et al., 2010) but did block the indirect target *hoxb9* (Domingos et al., 2001) (supplementary material Fig. S2B). Thus, these conditions induce neural tissue and posteriorize it via Wnt activation.

To screen for posterior neural genes, we harvested total RNA from animal caps treated with *noggin* alone (anterior neural), neuralized caps with activated TVGR (posteriorized neural), and neuralized animal caps treated with or without CHX prior to TVGR activation (enriched target sample). The RNAs from these samples were used for Illumina sequencing. The resulting reads were mapped to a collection of non-redundant full-length *Xenopus laevis* cDNA sequences (Xenopus Gene Collection, <http://xgc.ncbi.nih.gov>). By comparing read quantities between anterior neural tissue and tissue treated to enrich for direct targets, we found over 200 genes with expression that was increased greater than 2-fold (supplementary material Table S2). Importantly, the set included the direct targets *meis3* (Elkouby et al., 2010) and *cdx2* (Wang and Shashikant, 2007). To determine whether the expression of these genes was consistent with a posteriorizing Wnt signal, we stained *Xenopus tropicalis* embryos by *in situ* hybridization to identify candidates expressed in the posterior neurectoderm (Fig. 1A). Several candidates were expressed in dorsal tissues of gastrula embryos and posteriorly in early and mid-neurula stage embryos, consistent with the expression domains of known Wnt targets. Of particular note, the transcription factors *spalt-like 1* (*sall1*) and *sall4* showed strong expression in posterior neurectoderm (Fig. 1A).

We confirmed the results of our screen by qPCR (Fig. 1B). Incubation with CHX prior to activation of TVGR in neuralized caps resulted in increased *cdx2* (supplementary material Fig. S3A), *sall1* (supplementary material Fig. S4A) and *sall4* (Fig. 1B) expression. Incubation with CHX alone did result in an increase in *sall4* expression, but this was not statistically different from caps

treated with *noggin* alone. However, injection of *fgf8a* RNA [a posteriorizing spliceform of *fgf8* (Fletcher et al., 2006)] was sufficient to significantly induce *sall4* expression in neuralized animal caps (Fig. 1C).

The activation of *sall4* by TVGR in the presence of CHX prompted us to examine whether  $\beta$ -catenin binds to the genomic locus of *sall4*. We overexpressed a C-terminal FLAG-tagged version of *X. laevis*  $\beta$ -catenin and confirmed expression by immunoblotting (supplementary material Fig. S5A). Co-injection of FLAG-tagged  $\beta$ -catenin RNA restored dorsal structures in embryos injected with  $\beta$ -catenin morpholinos (MOs) (Heasman et al., 2000), demonstrating both the specificity and activity of this construct (supplementary material Fig. S2B). Consistent with a previous report (Yost et al., 1996), injection of 500 pg RNA encoding tagged  $\beta$ -catenin did not significantly alter dorsal structures as measured by the dorsoanterior index (Kao and Elinson, 1985) (supplementary material Fig. S2C). The *sall4* locus in *X. laevis* contains four exons and three introns (supplementary material Fig. S2D), with six putative TCF/LEF binding sites (Elkouby et al., 2010; McKendry et al., 1997) within the first intron (supplementary material Fig. S6). Three of these sites are tightly clustered within a 150 bp span at positions +2347, +2387 and +2456 (relative to the predicted transcription start site) and are conserved in *X. tropicalis*. Using FLAG antibodies for ChIP, this region was found to be significantly enriched compared with a negative control (*Xmhc2*) region (supplementary material Fig. S2E). A ~2.7 kb region upstream of *meis3* was used as a positive control for  $\beta$ -catenin binding (Elkouby et al., 2010). Anti-FLAG pulldowns in uninjected control embryos resulted in negligible enrichment of any loci assayed. A 500 bp fragment containing these three TCF/LCF sites was cloned and used in luciferase reporter assays. This fragment was not sufficient to enhance expression upon Wnt activation alone (supplementary material Fig. S2F) but was found to be significantly responsive to Fgf (Fig. 1D). Additional experiments demonstrated that Fgf and Wnt did not result in synergistic activation of this fragment.

Taken together, these results suggest that *sall4* is likely to be primarily regulated by the posterior Fgf signal and that Wnt signaling may play a minor or negligible role in its regulation.

### *sall4* and *sall1* expression in *X. laevis*

During gastrulation, *sall4* is expressed throughout the marginal zone and the animal pole (Fig. 2A). At stage 10, *sall4* is restricted to the sensorial neurectodermal cells in animal dorsal regions (Fig. 2E). At the onset of neurulation, *sall4* continues to be expressed in the sensorial neurectoderm (Fig. 2B,F,G). Neural expression of *sall4* in stage 15 (mid-neurula) embryos is in the hindbrain and spinal cord anlage (Fig. 2C,H,I). In later stage neurulae (stage 18), *sall4* spreads through the posterior neural tube, hindbrain, developing placodes and epidermis (Fig. 2D,J,K).

Similarly, *sall1* is expressed in the dorsal ectoderm and involuting mesoderm during gastrulation (supplementary material Fig. S4B,B'). Expression becomes restricted to the notochord and circumblastoporal collar at the early neurula stage (supplementary material Fig. S4C-C''). Like *sall4*, *sall1* is expressed in the spinal cord anlage at mid- and late neurula stages (supplementary material Fig. S4D-E'').

### Sall4 is required for posterior neural differentiation but not for induction or maintenance of neural identity

Given its neural expression, we hypothesized that loss of Sall4 would affect neural patterning. To test this, we knocked down Sall4 function with MOs. Morphant embryos had neural tube

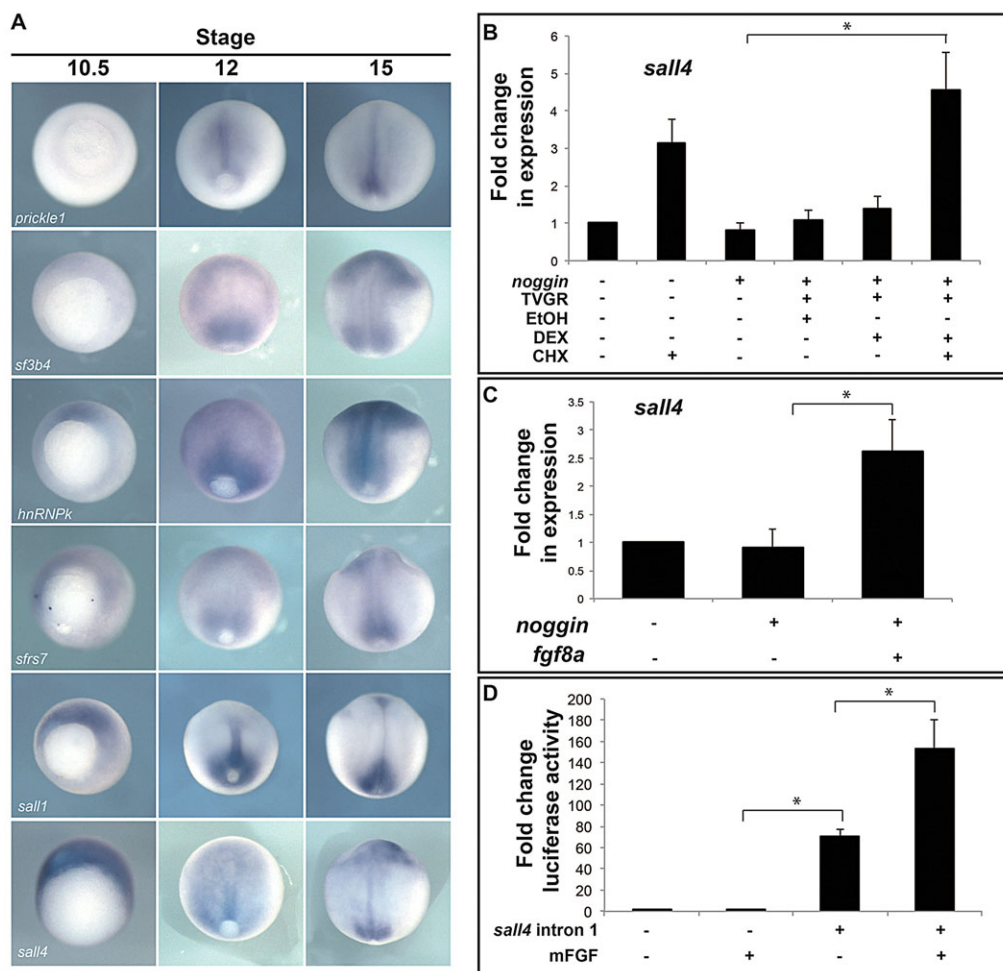


**Fig. 1. Expression screen for direct transcriptional targets of Wnt signaling in neural tissue.**  
**(A)** *X. tropicalis* embryos stained for transcripts identified as Wnt targets by RNA-seq. Stage 10.5 embryos show dorsoventral views with the dorsal lip toward the top. Stage 12 and 15 embryos show dorsal views with anterior toward the top.  
**(B,C)** qPCR on 15–25 animal caps treated as indicated on the x-axis. The y-axis shows expression relative to *odc*.  $n=4$  experiments.  
**(D)** Luciferase reporter assays in HEK293 cells treated with or without mouse Fgf.  $n=3$  experiments. Error bars indicate s.e.m. All means were compared by one-way ANOVA followed by Tukey post-hoc analyses (\* $P<0.05$ ).

closure defects and began to disintegrate at mid-tailbud stages. The closure defect is consistent with defects in neural patterning, so we assayed several markers of neural differentiation. The pan-neural marker *sox2* was expressed in the neural plate in uninjected and Sall4 morphants, demonstrating that the dorsal ectoderm of morphants still retained a neural identity (Fig. 3A,B). Conversely, the expression of *n-tub*, a marker for differentiating neurons, was markedly reduced although still present in the morphants,

suggesting that Sall4 is required for the second wave of neurogenesis in the tailbud tadpole (Fig. 3C,D). Another marker for early motor neuron differentiation, *nkx6.1*, was expressed in the central nervous system of morphants, and neural crest cells were still induced as determined by the expression of *snai2* (Fig. 3E,F). Although present, these markers were expressed in a pattern more similar to that of early neurulae, suggesting either a delay or failure of terminal differentiation. Sall4 morphants expressed the dorsal

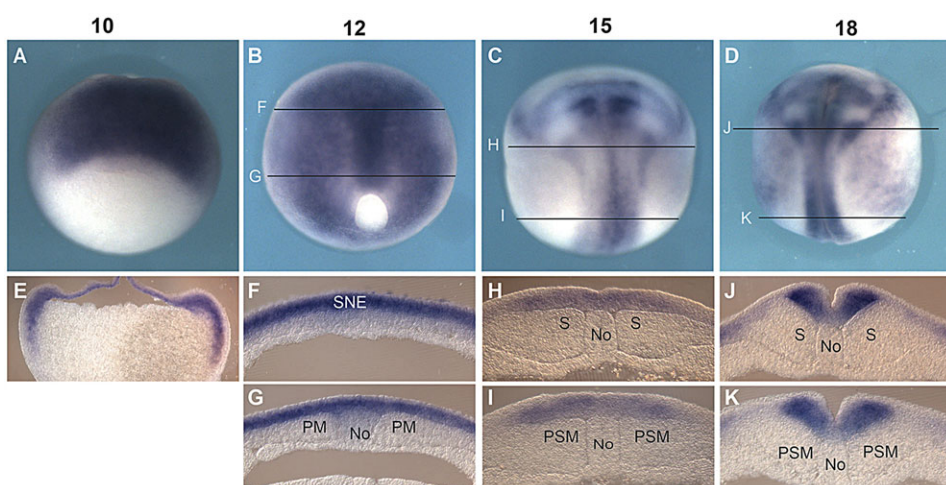


**Fig. 2. *sall4* is expressed in the neurectoderm.** (A) Stage 10 embryo stained for *sall4* RNA; dorsoventral view with the dorsal lip of the blastopore toward the top. (B–D) Dorsal views of neurula stage embryos with anterior toward the top. (E) Sagittal section of stage 10 embryo stained for *sall4* expression; animal pole is to the top and dorsal to the right. (F–K) Transverse sections at anterior (F,H,J) or posterior (G,I,K) of embryos stained for *sall4* as indicated in B–D. (E–K) 50  $\mu$ m sections, with (F–K) dorsal uppermost. SNE, sensorial neurectoderm; No, notochord; S, somite; PM, paraxial mesoderm; PSM, presomitic mesoderm.

mesoderm marker *myoD* in a similar pattern to uninjected control embryos, and therefore the neural defects were not secondarily due to a loss of paraxial mesoderm (Fig. 3G,H).

As *sall4* was identified in a screen for posterior neural genes, we predicted that Sall4 morphants would lose posterior neural identity. To test for this, we injected Sall4 MOs into one animal dorsal (A/D) cell of 4-cell stage embryos to allow for comparison between injected and uninjected sides. The injected side of embryos showed a posterior shift in expression of the hindbrain markers *gbx2* (Fig. 4A,B), *mafb* (Fig. 4D,E) and *pax2* (Fig. 4J,K). Sall4 loss resulted in loss of *meis3* rhombomere expression and a reduction of its spinal cord expression domain (Fig. 4L). Surprisingly, overexpression of *sall4* did not result in a change or shift in any of these markers (Fig. 4C,F,I,L), nor was it sufficient to rescue defects associated with Dkk1 overexpression (supplementary material Fig. S7).

The posterior shift of brain markers observed in Sall4 morphants suggested that knockdown of Sall4 results in an expansion of anterior neural identity at the expense of posterior neural differentiation. Accordingly, *otx2* is expanded and *krox20* is significantly shifted relative to the control side (Fig. 5A-C). Strikingly, the injected side had a significant reduction in the expression domain of the spinal cord markers *hoxb9* (Fig. 5D-F), *hoxc10* (Fig. 5G-I) and *hoxd10*

(Fig. 5J-L). However, Sall4 knockdown does not reduce expression of the Wnt target *cdx2* to the same extent (supplementary material Fig. S3B,C).

### Loss of Sall4 in the neural plate increases expression of the Pou5f1 homologs *pou5f3.1*, *pou5f3.2* and *pou5f3.3*

The failure of Sall4 morphants to induce posterior neural identity suggested that the caudal tissue remained in an undifferentiated state. In mouse embryos, Sall4 positively regulates the stem cell factor *Pou5f1* (*Otx4*) to maintain pluripotency (Zhang et al., 2006). One explanation for our results is that Sall4 negatively regulates the *Pou5f1* homologs in neural tissue. In *Xenopus*, there are three class 5 Pou-domain genes that show similar sequence and ancient synteny to mammalian *Pou5f1* (Morrison and Brickman, 2006). However, eutherian mammals and frogs retain different copies of the locus from the last tetrapod whole-genome duplication, and their Pou5 genes are not the simple orthologs of *Pou5f1*. Here, we use the term *pou5f3* (as used by Xenbase.org, zfin.org) (Morrison and Brickman, 2006; Frankenberg et al., 2010).

If Sall4 negatively regulates *pou5f3*, then morphants should increase their expression. Indeed, knockdown of Sall4 in unilateral and bilateral injections resulted in ectopic expression of *pou5f3.2* (*oct25*) (Fig. 6A-C), *pou5f3.3* (*oct60*) (Fig. 6D-F)

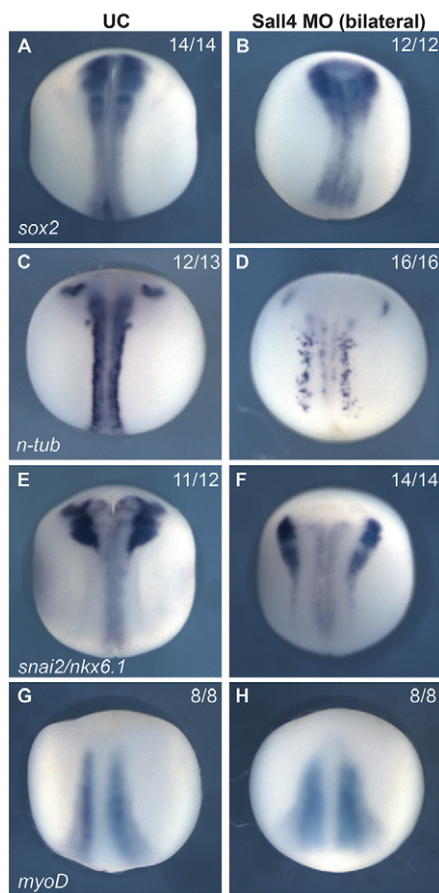


**Fig. 3. Loss of Sall4 results in a loss of neural differentiation.**

Whole-mount *in situ* hybridizations of (A,C,E,G) uninjected control (UC) embryos and (B,D,F,H) embryos injected bilaterally with 40 ng Sall4 MO (20 ng/blastomere at the 2-cell stage), showing expression of *sox2* (A,B), *n-tub* (C,D), *snai2* and *nkx6.1* (E,F) and *myoD* (G,H). Dorsal views with anterior to the top. The number of embryos showing the illustrated expression pattern among the total examined is indicated top right.

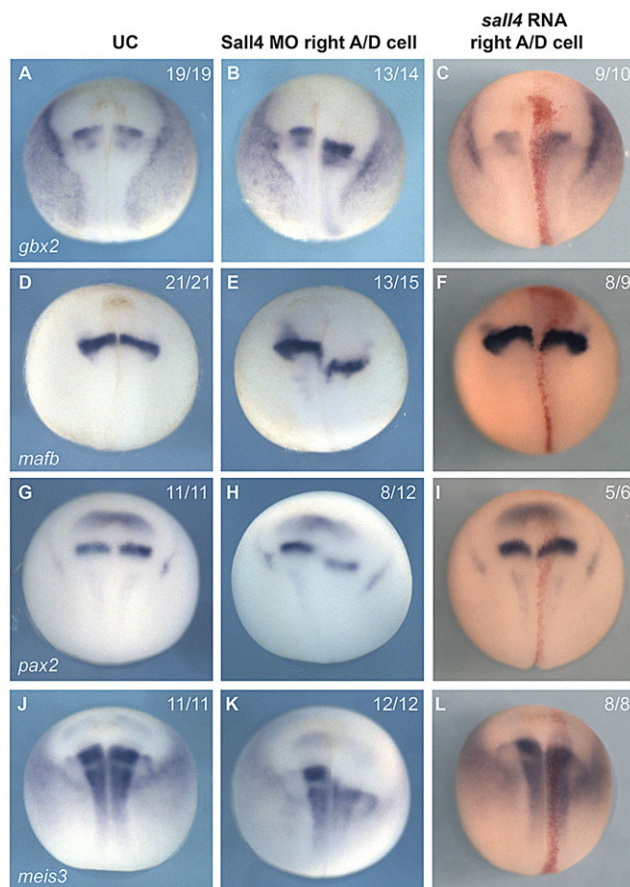


**Fig. 4. Expression of hindbrain markers is altered in Sall4 morphants.**

Whole-mount *in situ* hybridizations of (A,D,G,J) uninjected control embryos, (B,E,H,K) embryos injected with 20 ng Sall4 MO into the right animal-dorsal (A/D) blastomere, and (C,F,I,L) embryos injected with 250 pg *sall4* RNA into the right A/D blastomere, showing expression of *gbx2* (A-C), *mafb* (D-F), *pax2* (G-I) and *meis3* (J-L). Dorsal views with anterior to the top.

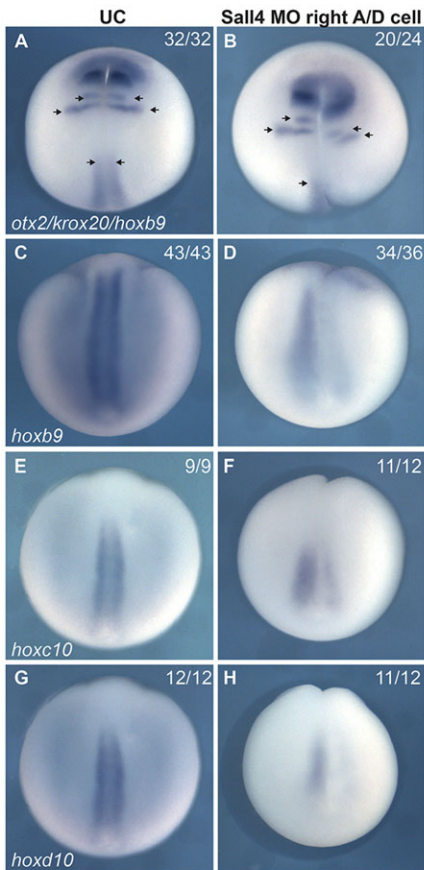


**Fig. 5. Sall4 knockdown results in a loss of spinal cord differentiation.** (A–H) Whole-mount *in situ* hybridization of (A,C,E,G) uninjected control embryos and (B,D,F,G) embryos injected with 20 ng Sall4 MO into the right A/D blastomere. (A,B) Expression of *otx2*, *krox20* and *hoxb9*. Arrows indicate the relative anterior-posterior (A–P) position of *krox20* and the anterior limit of *hoxb9*. Dorsal views with anterior to the top. (C–H) Posterior views of *hoxb9* (C,D), *hoxc10* (E,F) and *hoxd10* (G,H) expression. (I–L) Quantification of A–P patterning defects associated with Sall4 knockdown. (I) Distance between the anteriormost expression of *otx2* and the first *krox20* stripe in arbitrary units (AU). (J–L) Length of the *hoxb9* (J), *hoxc10* (K) and *hoxd10* (L) expression domains (AU). Error bars indicate s.e.m. Means were compared between left and right sides by Student's *t*-test (\**P*<0.05, \*\**P*<0.01, \*\*\**P*<0.001). Data were generated from analyzing all embryos shown in A–H.

and *pou5f3.1* (*oct91*) (Fig. 6G–I). Accordingly, the increase in expression of *pou5f3.2* and *pou5f3.1* was greatest in the neural tube, where *sall4* is normally expressed. *pou5f3* expression in Sall4 morphants relative to control embryos was quantified by qPCR and displayed a significant increase in all three *pou5f3* genes (Fig. 6J–L). Co-injection of *X. tropicalis* *sall4* RNA that is not targeted by the Sall4 MO resulted in a partial rescue of the *pou5f3.2* expression level and a full rescue of the *pou5f3.3* and *pou5f3.1* expression levels.

Next, we asked whether ectopic *pou5f3* expression is sufficient to block posterior neural differentiation by injecting RNA for the three *pou5f3* genes unilaterally into embryos and assaying A–P neural gene expression. Neural plate cells expressing ectopic *pou5f3* (as traced by β-galactosidase) had altered *otx2* expression and failed to express *krox20* (Fig. 7A,B), *hoxb9* (Fig. 7C,D) and *hoxc10* (Fig. 7E,F). This loss in A–P neural marker expression cannot be attributed to a loss of neural identity as the *pou5f3*-injected side of embryos broadly expresses *sox2* (Fig. 7G,H).

#### The loss of spinal cord identity in Sall4 morphants is attributable to the overexpression of *pou5f3*

The observed *pou5f3* increase following knockdown of Sall4 suggested a mechanism for the loss of posterior neural identity whereby the ectopic *pou5f3* expression prevents differentiation of neural tissue into spinal cord. We reasoned that knocking down *pou5f3* in Sall4 morphants would restore posterior neural identity. To this end, we co-injected MOs targeting the three *pou5f3* homologs (Morrison and Brickman, 2006; Livigni et al., 2013) along with Sall4 MOs. Consistent with the results described above, knockdown of Sall4 resulted in loss of posterior *hoxb9* (Fig. 8A,E),

*hoxc10* (Fig. 8B,F) and *hoxd10* (Fig. 8C,G) but not in a loss of pan-neuronal *sox2* (Fig. 8D,H). Co-injection of the Pou5f3 MOs with Sall4 MOs restored the spinal cord marker expression lost by Sall4 knockdown alone (Fig. 8I–K). Knockdown of Pou5f3 in Sall4 morphants did not restore *krox20* stripe expression, consistent with previous work showing that Pou5f3 MOs inhibit *krox20* expression (Morrison and Brickman, 2006). Although reduced, *sox2* was expressed in the neural plate of Pou5f3 morphants (Fig. 8N) and Sall4-Pou5f3 double morphants (Fig. 8L). Finally, measuring the Hox gene expression domains of Sall4 and Sall4-Pou5f3 morphants revealed a significant rescue of all three spinal cord markers (Fig. 8M).

#### Sall4 is required for neural posteriorization by the caudalizing factors Fgf and RA

Our results demonstrate that posteriorizing factors induce Sall4 expression, which represses *pou5f3*, thereby allowing posterior neural differentiation. Fgf and RA signaling also posteriorize the neural plate. Therefore, we tested whether repression of *pou5f3* via Sall4 is required for both Fgf- and RA-induced caudalization. We treated embryos with either *fgf8a* RNA or incubation in RA. Again, Sall4 knockdown resulted in loss of *hoxb9* (Fig. 9A,B) without major alterations to *sox2* (Fig. 9E,F). Overexpression of *fgf8a* in the dorsal ectoderm resulted in expansion of *sox2* and *hoxb9*, a lateral expansion of *krox20*, and repression of *otx2* (Fig. 9C) (Fletcher et al., 2006). These expansions are due to the long-range effects of overexpressing the secreted Fgf ligand. However, overexpressing *fgf8a* in Sall4 morphants still resulted in *otx2* (brain) repression, but *hoxb9* (spinal cord) was lost (Fig. 9D). *krox20* expression in rhombomere 5 was severely reduced in the Sall4 morphants despite *fgf8a* overexpression,

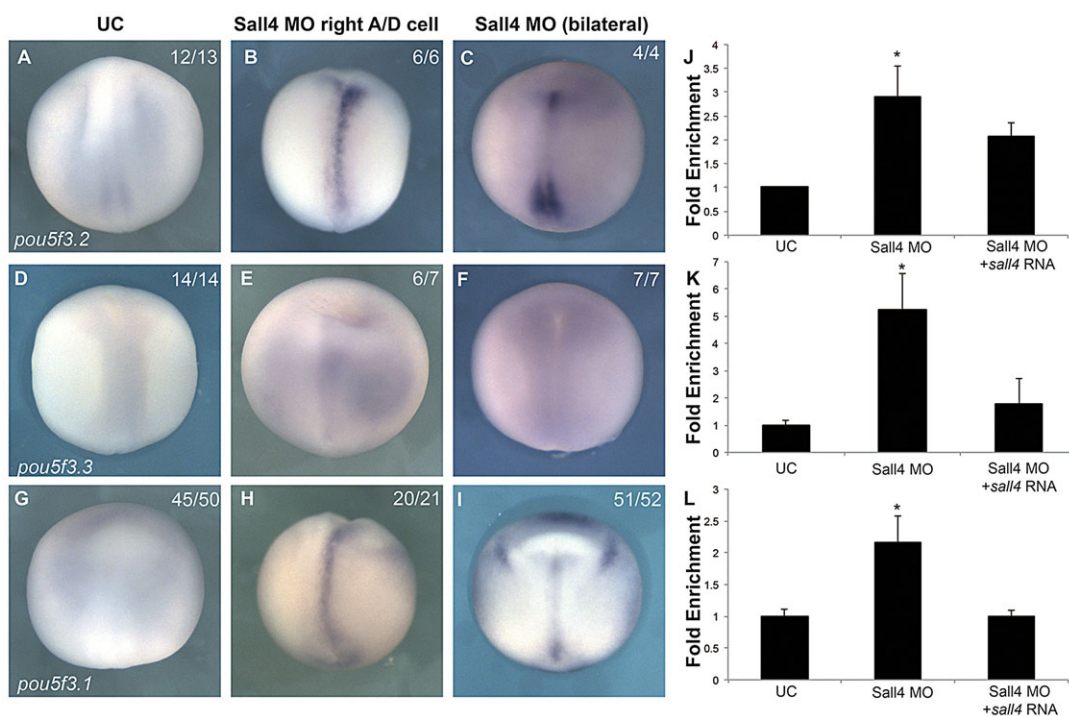


**Fig. 6. Knockdown of Sall4 causes an increase in *pou5f3* expression.** (A–I) Whole-mount *in situ* hybridization of (A,D,G) uninjected control embryos, (B,E,H) embryos injected with 20 ng Sall4 MO into the right A/D blastomere, and (C,F,I) embryos injected bilaterally with 40 ng Sall4 MO (20 ng/blastomere at the 2-cell stage), showing expression of (A–C) *pou5f3.2*, (D–F) *pou5f3.3* and (G–I) *pou5f3.1*. Dorsal views, anterior to the top. (J–L) qPCR for *pou5f3.2* (J), *pou5f3.3* (K) or *pou5f3.1* (L) in uninjected embryos, embryos injected with 40 ng Sall4 MO (20 ng/blastomere at the 2-cell stage), and embryos injected with 40 ng Sall4 MO (20 ng/blastomere at the 2-cell stage) plus 500 pg *X. tropicalis* *sall4* RNA (250 pg/animal-dorsal blastomere at the 4-cell stage). The expression is relative to *odc*. Error bars indicate s.e.m. Means compared with uninjected control by one-way ANOVA followed by Tukey post-hoc analyses (\*P<0.05). n=4 experiments.

whereas rhombomere 3 expression remained expanded, probably owing to the specific posteriorizing effects of Sall4. Morphants typically had a posterior shift and reduction in rhombomere 5 *krox20* expression, whereas expression in rhombomere 3 was shifted but not reduced (Fig. 5B).

Increasing RA signaling results in severe loss of anterior neural tissue and expansion of posterior identities (Durston et al., 1989; Sive et al., 1990; Ruiz i Altaba and Jessell, 1991; Blumberg et al., 1997; Shiotsugu et al., 2004). To test whether Sall4 is required for posteriorization via RA, we treated control embryos and Sall4 morphants with all-trans retinoic acid (ATRA). Uninjected control embryos treated with 1 μM ATRA lacked *otx2* and *krox20* but sustained *hoxb9* expression (Fig. 9I). However, 1 μM ATRA treatment of Sall4 morphant embryos repressed *otx2* and *krox20* but also failed to induce the caudally expressed marker *hoxb9* (Fig. 9J). The reduction of these markers was not due to a loss of neural tissue as *sox2* expression was similar between control embryos, embryos treated with ATRA, and Sall4 morphant embryos treated with ATRA (Fig. 9E,K,L).

## DISCUSSION

Wnt, Fgf and RA signaling are caudalizing factors required for posteriorization of the neural plate. However, the transcription factors identified as mediating the patterning signals from these pathways have largely been restricted to those specifying midbrain and hindbrain fates. In this study, we identify *sall4* as a posteriorizing factor target required for spinal cord differentiation. The primary role of Sall4 in neural patterning is to repress *pou5f3* (*oct4*). This repression is necessary for spinal cord differentiation; Sall4 knockdown (Fig. 5E,H,K), as well as *pou5f3* overexpression

(Fig. 7D,F), results in loss of spinal cord fate. Furthermore, the posterior defects in Sall4 morphants can be rescued via *pou5f3* knockdown (Fig. 8I–K). We suggest that repression of *pou5f3* via Sall4 provides a permissive environment allowing cells in the neural plate to respond to instructive signals from Fgf, RA and Wnt. This model fits with the observation that overexpression of *sall4* did not result in a perturbation of A–P hindbrain marker expression (Fig. 4). If the main role of Sall4 in neural patterning is to repress *pou5f3*, then overexpression is unlikely to have a significant effect on otherwise normal embryos. Further, this model predicts that Sall4 would not rescue a Wnt loss-of-function phenotype since it is functioning as a permissive and not as an instructive signal. Another prediction is that Sall4 is required for adoption of posterior fates by multiple posteriorizing signals. Therefore, an increase in *pou5f3* expression after Sall4 knockdown would inhibit differentiation induced by other caudalizing factors. Indeed, we found Sall4 knockdown prevented induction of *hoxb9* by Fgf or RA (Fig. 9D,J).

Our findings build upon previously described mechanisms of posterior neural patterning. Wnt activates *cdx1* (Prinos et al., 2001; Pilon et al., 2007) and, in frogs, Cdx1 represses *pou5f3* gene expression at the onset of gastrulation (Rousso et al., 2011). However, knockdown of Cdx1 does not result in a loss of spinal cord differentiation, and combinatorial knockdown of Cdx1/2/4 is required before *hoxb9* and *hoxc10* are reduced (Faas and Isaacs, 2009). There is, however, a dramatic loss of *hoxb9*, *hoxc10* and *hoxd10* in Sall4 morphants. In the absence of Sall4, *pou5f3* expression remains high, resulting in neural cells being unable to commit to a posterior neural fate and differentiate into spinal cord. Several studies have shown that Cdx factors regulate posterior Hox gene expression in vertebrates (Isaacs et al., 1998; van den

Akker et al., 2002; Gaunt et al., 2004, 2008). Therefore, Wnt acts as an instructive signal through the activation of Cdx genes to induce posterior Hox genes and thereby transform the neural precursors into a posterior fate. Here, we find that *sall4* represses *pou5f3*, providing a parallel, permissive signal for posterior Hox gene expression. Wnt still signals in the posterior neural regions of Sall4 morphants, activating Cdx genes (supplementary material Fig. S3B,C), but the prolonged expression of *pou5f3* prevents Hox gene expression. Conversely, it is likely that *sall4* is still expressed in Cdx morphants, priming the neural plate to respond to other instructive signals. This could explain why knockdown of individual Cdx homologs results in unexpectedly mild phenotypes.

#### Posteriorizing signals regulate *sall4* expression

Our work found *sall4* to be activated by Fgf signaling in the neurectoderm. However, our finding that a 500 bp fragment in the first intron of *sall4* is enriched in β-catenin ChIP is consistent with it being a Wnt target (supplementary material Fig. S2E). However, this region does not mediate a Wnt-induced signal. Interestingly, we found that this region does show responsiveness to Fgf signaling. Taken together, these experiments show that Fgf is the primary posteriorizing signal that regulates *sall4* expression and that Wnt either plays a minor role or does not regulate *sall4* during early neural patterning.

The broad expression of *sall4* at early neurula stages (Fig. 2B) and later in limbs during *Xenopus* development and regeneration (Neff et al., 2011) suggests regulation through different enhancers, each responsible for discrete expression domains. This is the case with the neural expression of Sox2 in the chick, which is regulated by five different enhancers, each responsible for a portion of the full expression domain (Uchikawa et al., 2003). Fgf signaling is sufficient to posteriorize neurectoderm (Kengaku and Okamoto, 1995; Lamb and Harland, 1995; Christen and Slack, 1997; Fletcher et al., 2006), and we found that this activity requires Sall4. Therefore, it is possible that Fgf and Wnt signaling converge on other, as yet unidentified, enhancers to regulate *sall4* expression. Indeed, Fgf and Wnt signaling converge on one enhancer in the chick *sox2* gene to mediate the most posterior expression of *sox2* in the neural plate (Takemoto et al., 2006). Likewise, Wnt and Fgf response elements in the enhancers of *pax3* and *zic* genes cooperatively regulate their expression (Garnett et al., 2012), and both pathways mediate expression of these genes at the neural plate border (Monsoro-Burq et al., 2005).

#### A-P neural patterning requires downregulation of pluripotency factors

In amphibians, caudalization of the neural plate via Fgf and canonical Wnt signaling induces undifferentiated neural precursors to commit to posterior fates. This induction requires repression of stem cell factors and the activation of differentiation factors. *pou5f3* (*oct4*) genes are first expressed animalily in cleavage stages and throughout the mesoderm and ectoderm of amphibian gastrulae (Frank and Harland, 1992; Morrison and Brickman, 2006). Knockdown of Pou91 (Pou5f3.1), Pou60 (Pou5f3.3) and Pou25 (Pou5f3.2) results in precocious cell fate commitment in the three germ layers (Morrison and Brickman, 2006; Snir et al., 2006). Accordingly, *pou5f3* overexpression prolongs the undifferentiated state (Morrison and Brickman, 2006; Archer et al., 2011). Our results suggest that *pou5f3* expression must be downregulated in the neurectoderm to allow for cells to respond to instructive Wnt/Fgf/RA signals and commit to posterior fates.

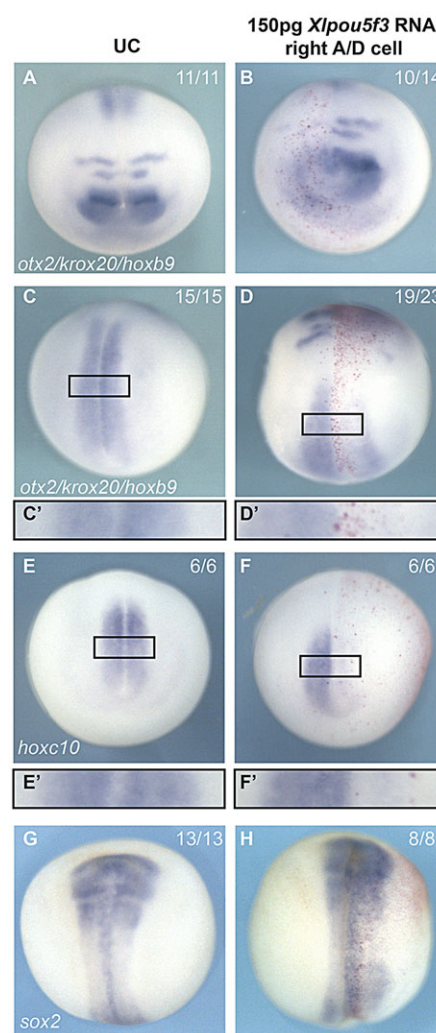


**Fig. 7. Overexpression of *pou5f3* represses neural differentiation.**

Whole-mount *in situ* hybridization of (A,C,E,G) uninjected control embryos and (B,D,F,H) embryos injected with 150 pg *pou5f3* RNA (50 pg each of *pou5f3.2*, *pou5f3.3* and *pou5f3.1* RNAs) into the right A/D blastomere. Red staining is β-galactosidase used as a tracer for RNA injection. (C'-F') Higher magnification views of the boxed regions in C-F. (A-D) *otx2*, *krox20* and *hoxb9* expression in anterior (A,B) or dorsal (C,D) view. (E-H) *hoxc10* (E,F) and *sox2* (G,H) expression in dorsal view.

Several studies have demonstrated the role for the *pou5f3* genes in maintaining pluripotency in *Xenopus*. In the early embryo, Oct25 (Pou5f3.2) and Oct60 (Pou5f3.3) were found to antagonize VegT and Wnt/β-catenin signaling to prevent precocious germ layer fates (Cao et al., 2007) and overexpression of Oct25 activates *Xvent-2B*, resulting in a failure of neurectoderm to differentiate (Cao et al., 2004). Further, the histone methyltransferase Suv4-20h has been demonstrated to directly repress *oct25* to allow for neural differentiation in *Xenopus* eye development (Nicetto et al., 2013). These studies all support a conserved role of *pou5f3* genes in pluripotency (Morrison and Brickman, 2006; Cao et al., 2007). Our results are consistent with the model; we find that the ectopic expression of *pou5f3* following knockdown of Sall4 results in the neurectoderm failing to differentiate in response to transforming signals.

Injection of *pou5f3* RNA results in more severe anterior defects than does Sall4 knockdown. This is likely to be due to higher levels of *pou5f3* expression following RNA injection (Fig. 7). Indeed, since the Pou5f3 family inhibits Fgf signaling (Cao et al., 2006; Snir

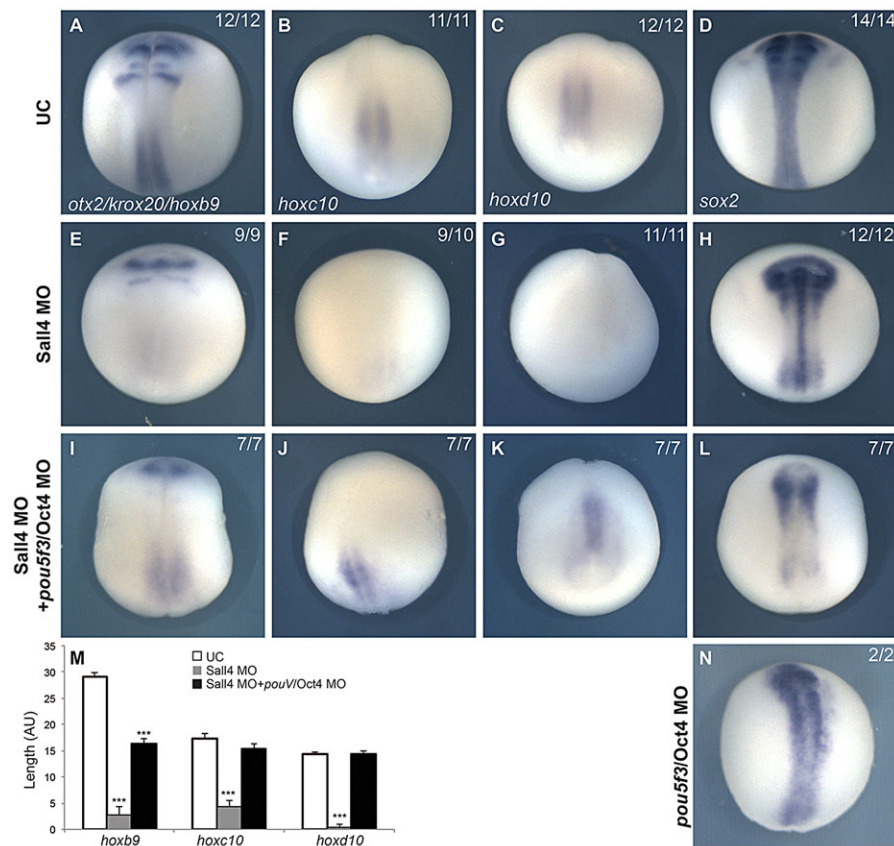


**Fig. 8. Loss of spinal cord in *Sall4* morphants due to an increase in *pou5f3* expression.**  
 (A-L) Whole-mount *in situ* hybridization of (A-D) uninjected control embryos, (E-H) embryos injected with 40 ng *Sall4* MO (20 ng/blastomere at the 2-cell stage), or (I-L) embryos injected with 40 ng *Sall4* MO, 20 ng *Pou5f3.2* MO, 10 ng *Pou5f3.3a* MO, 10 ng *Pou5f3.3b* MO, and 20 ng *Pou5f3.1* MO. (N) Embryos injected with 20 ng *Pou5f3.2* MO, 10 ng *Pou5f3.3a* MO, 10 ng *Pou5f3.3b* MO and 20 ng *Pou5f3.1* MO. Expression is shown for (A,E,I) *otx2*, *krox20* and *hoxb9*, (B,F,J) *hoxc10*, (C,G,K) *hoxd10* and (D,H,L,N) *sox2*. Dorsal views with anterior to the top. (M) Quantification of posterior neural gene expression as measured by expression domain length in arbitrary units (AU). White, uninjected control embryos. Gray, embryos injected with 40 ng *Sall4* MO (20 ng/blastomere at the 2-cell stage). Black, embryos injected with 40 ng *Sall4* MO, 20 ng *Pou5f3.2* MO, 10 ng *Pou5f3.3a* MO, 10 ng *Pou5f3.3b* MO and 20 ng *Pou5f3.1* MO. Error bars indicate s.e.m. Means compared with uninjected control by one-way ANOVA followed by Tukey post-hoc analyses (\*\* $P < 0.001$ ). Data were generated from analyzing all embryos shown in A-C, E-G, and I-K.

et al., 2006), the disruption of *krox20* expression in the *pou5f3*-injected embryos is likely to be due to ectopic Pou5f3 inhibiting hindbrain patterning mediated by Fgf from the isthmus.

The class 5 Pou-domain factors play a conserved role in maintaining pluripotency in *Xenopus*. Here, we show that Sall4 mediates the transition between pluripotency maintenance and differentiation in the neural plate via repression of *pou5f3*. How Sall4 regulates *pou5f3* and whether this is a general role for Sall4 or specific to the neurectoderm remains to be elucidated.

## MATERIALS AND METHODS

#### **EMBRYOS AND EXPLANT CULTURE**

*X. laevis* embryos were obtained (Sive et al., 2010) and staged (Nieuwkoop and Faber, 1967) as described previously. Ectodermal explants (animal caps) were cut using fine watchmaker's forceps from stage 9 embryos and cultured in  $0.75 \times$  NAM (Sive et al., 2010).

## Cloning and DNA constructs

A cDNA clone of *X. tropicalis* *sall4* (CT025472) was identified in a full-length cDNA collection generated from gastrula embryos (Gilchrist et al., 2004). The coding sequence was subcloned into CS-108 (DQ649433.1) with *Sall* and *XhoI* using primers (5'-3'): forward, CGATGTCGACGGACCATG-TCGAGGCAGAACGCC; and reverse, ATCGATCCTCGAGTTA-cttacgtcgatcacttgtaaatcGTTCACCGCAATATTTT. The coding sequence of *X. laevis*  $\beta$ -catenin was amplified with a FLAG epitope using: forward, GCATGAATTCCCACCATTGGCAACTCAAGCAGATCT; and reverse, GCTAGCGGCCGCTTAActtacgtcgatcacttgtaaatcCAAGTCAGTGTCAA-CCAGG; it was then subcloned into CS-108 with *EcoRI* and *NotI*. Lowercase sequence delineates the FLAG epitope and underlined sequences are restriction sites. *X. laevis* *sall4* was PCR amplified with primers: forward, CTTGGTGCGCACTTATCTCA; and reverse, GCCTCAGATTGTGTGG-GACT; it was then cloned into pCR TOPO II (Invitrogen) for the generation of antisense RNA probes.

## **RNA and MO microinjections**

Capped RNAs were synthesized using mMessage mMachine (Ambion). *sall4* CS-108, *fgf8a* CS-108, *noggin* CS-108 and  $\beta$ -catenin CS-108 were linearized with *Asc*I and transcribed with SP6 RNA polymerase. The *pou5f3* plasmids (a gift from Joshua Brickman, University of Copenhagen), TVGR (Darken and Wilson, 2001) and nuclear  $\beta$ -galactosidase CS2+ were linearized with *Not*I and transcribed with SP6. All RNAs were injected in 5 or 10 nl bursts along with *GFP* and *lacZ* RNAs, which served as tracers.

The Sall4 MO oligonucleotide (5'-GCCAATTATCCCTTCTCCAC-AC-3'; Gene Tools) and the Pou5f3 MOs (a gift from Joshua Brickman) (Livigni et al., 2013; Morrison and Brickman, 2006) were injected in 5 or 10 nl along with fluoresceinated control MO (Gene Tools) to serve as a tracer.

## Cycloheximide and dexamethasone treatments

*noggin* (10 pg) and TVGR (4 pg), an inducible Wnt agonist (Darken and Wilson, 2001), RNAs were injected animalily into both blastomeres of 2-cell embryos (Fig. 1A). At stage 9, animal caps were cultured with or without 10  $\mu$ M dexamethasone (DEX) (Sigma) to activate Wnt signaling (Darken and Wilson, 2001). To block translation, caps were pre-treated with 5  $\mu$ M cycloheximide (CHX) (Sigma) for 1.5 h prior to DEX addition (Obrig et al., 1971). Animal caps were cultured until stage 15 equivalent and total RNA was harvested using Trizol (Invitrogen).

## Whole-mount *in situ* hybridization

Embryos were stained by *in situ* hybridization as described (Harland, 1991). β-galactosidase staining was as described (Fletcher et al., 2006). Embryos for sectioning were mounted in a PBS solution containing 20% sucrose, 30% BSA and 4.9% gelatin, and fixed with 1.5% glutaraldehyde. Embedded embryos were sectioned on a Pelco 101 vibratome.

RT-PCR and qPCR

RNA was isolated from whole embryos or animal caps using Trizol and 1 µg total RNA was reverse transcribed with either MMLV reverse transcriptase

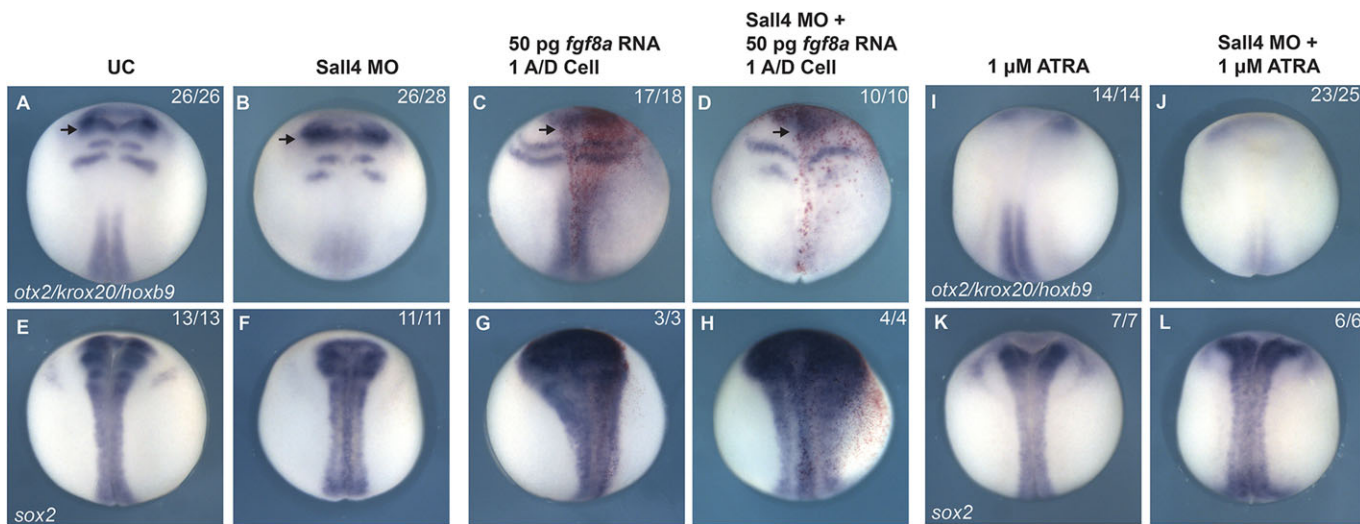


**Fig. 9. Fgf and RA signaling fail to posteriorize Sall4 morphants.** Whole-mount *in situ* hybridization of (A,E) uninjected control embryos, (B,F) embryos injected with 40 ng Sall4 MO (20 ng/blastomere at the 2-cell stage), (C,G) embryos injected with 50 pg *fgf8a* RNA into the right A/D blastomere, (D,H) embryos injected with 40 ng Sall4 MO (20 ng/blastomere at the 2-cell stage) and 50 pg *fgf8a* RNA into the right A/D blastomere, (I,K) embryos treated with 1 μM all-trans retinoic acid (ATRA) and (J,L) embryos injected with 40 ng Sall4 MO (20 ng/blastomere at the 2-cell stage) and treated with 1 μM ATRA. Expression is shown for (A–D,I,J) *otx2*, *krox20* and *hoxb9* or (E–H,K,L) *sox2*. Arrowheads indicate the posterior limit of *otx2* expression. Dorsal views, anterior to the top.

(Promega) for semi-quantitative PCR or iScript (Bio-Rad) for quantitative PCR (qPCR). Semi-quantitative PCRs included [<sup>32</sup>P]dCTP (PerkinElmer) in the reaction and were analyzed during the log phase of amplification. qPCR reactions were amplified on a CFX96 light cycler (Bio-Rad). *ornithine decarboxylase* (*odc*) and *elongation factor 1α1* (*eef1α1*) were used for internal controls. All primers annealed at 60°C and are listed in supplementary material Table S1.

#### RNA-seq

RNA-seq was performed as described (Dichmann and Harland, 2012). Single-end 76-bp reads were sequenced on an Illumina Genome Analyzer II. All reads were mapped to an index created from a collection of full-length *X. laevis* mRNA sequences (NCBI, <http://xgc.nci.nih.gov>) using TOPHAT and BOWTIE (Langmead et al., 2009; Trapnell et al., 2009). Analysis of transcript abundance employed CUFFDIFF (Trapnell et al., 2010).

#### Chromatin immunoprecipitation (ChIP)

FLAG-β-catenin RNA-injected embryos were prepared for ChIP as described (Blythe et al., 2009). Chromatin shearing used a Branson Model 450 digital sonifier with a Model 102C probe for 24 ten-second bursts set at 30% amplitude. ChIP DNA was quantified with SYBR Green PCR mix (Bio-Rad) on a CFX96 light cycler (Bio-Rad). Enrichment was calculated by comparing the percentage input among ChIP samples. Uninjected embryos served as a control for non-specific binding. *Xmhc2* (Blythe et al., 2009) and  *meis3* (Elkouby et al., 2010) served as negative and positive controls, respectively, for β-catenin binding.

#### Luciferase assays and mutagenesis

A 500 bp fragment containing three putative TCF/LEF sites in *sall4* intron 1 (Scaffold 1115: 234, 269–234, 644) was cloned into the pGL4.23 luciferase reporter (Promega) with *SacI* and *XhoI* (NEB). Each of the three sites was mutagenized using *Pfx* polymerase (Invitrogen) according to the manufacturer's instructions. HEK293 cells were transfected with 0.1 μg each of pGL4.23 and pLR-CMV (Promega) and treated with 0.1 μg mouse Fgf or 50 μM BIO (Cayman). Relative luciferase units were measured on a Turner Design TD-20/20 luminometer using the Dual Luciferase Assay Kit (Promega).

#### Acknowledgements

We thank Joshua Brickman for the Pou5f3 MOs and plasmids; Elena Casey for the *pou91* clone; Rakhi Gupta and Julie Baker for technical assistance with ChIP; and Darwin Dichman and Sofia Medina-Ruiz for computational assistance.

#### Competing interests

The authors declare no competing financial interests.

#### Author contributions

J.J.Y. and R.M.H. designed the experiments with contributions from R.A.S.K. and N.R.K. J.J.Y., R.A.S.K., N.R.K. and S.D.M. carried out all experiments. J.J.Y., R.A.S.K., N.R.K., S.D.M. and R.M.H. analyzed all data generated from the experiments. J.J.Y. and R.M.H. wrote the paper incorporating comments from R.A.S.K., N.R.K. and S.D.M.

#### Funding

This work was supported by a National Institutes of Health grant [GM42341] to R.M.H. Deposited in PMC for release after 12 months.

#### Supplementary material

Supplementary material available online at <http://dev.biologists.org/lookup/suppl/doi:10.1242/dev.099374/-DC1>

#### References

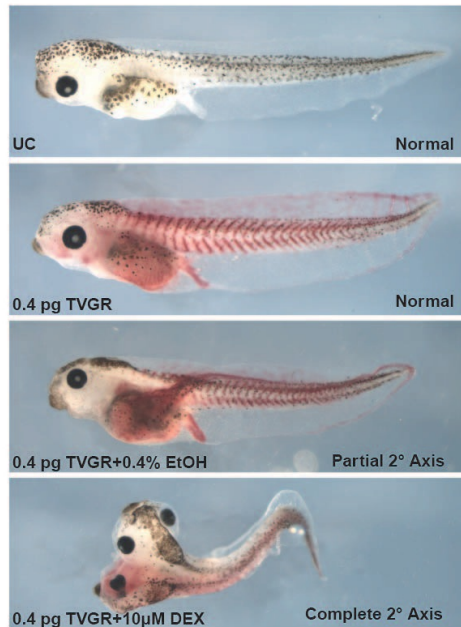
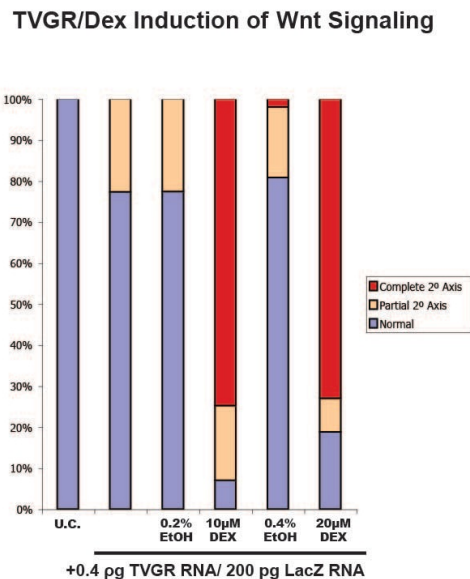
- Archer, T. C., Jin, J. and Casey, E. S. (2011). Interaction of Sox1, Sox2, Sox3 and Oct4 during primary neurogenesis. *Dev. Biol.* **350**, 429–440.
- Blumberg, B., Bolado, J., Moreno, T. A., Kintner, C., Evans, R. M. and Papalopulu, N. (1997). An essential role for retinoid signaling in anteroposterior neural patterning. *Development* **124**, 373–379.
- Blythe, S. A., Reid, C. D., Kessler, D. S. and Klein, P. S. (2009). Chromatin immunoprecipitation in early *Xenopus laevis* embryos. *Dev. Dyn.* **238**, 1422–1432.
- Böhm, J., Buck, A., Borozdin, W., Mannan, A. U., Matysiak-Scholze, U., Adham, I., Schulz-Schaeffer, W., Floss, T., Wurst, W., Kohlhase, J. et al. (2008). *Sall1*, *sall2*, and *sall4* are required for neural tube closure in mice. *Am. J. Pathol.* **173**, 1455–1463.
- Cao, Y., Knöchel, S., Donow, C., Miethe, J., Kaufmann, E. and Knöchel, W. (2004). The POU factor Oct-25 regulates the Xvent-2B gene and counteracts terminal differentiation in *Xenopus* embryos. *J. Biol. Chem.* **279**, 43735–43743.
- Cao, Y., Siegel, D. and Knöchel, W. (2006). Xenopus POU factors of subclass V inhibit activin/nodal signaling during gastrulation. *Mech. Dev.* **123**, 614–625.
- Cao, Y., Siegel, D., Donow, C., Knöchel, S., Yuan, L. and Knöchel, W. (2007). POU-V factors antagonize maternal VegT activity and beta-Catenin signaling in *Xenopus* embryos. *EMBO J.* **26**, 2942–2954.
- de Celis, J. F. and Barrio, R. (2009). Regulation and function of Spalt proteins during animal development. *Int. J. Dev. Biol.* **53**, 1385–1398.
- Christen, B. and Slack, J. M. W. (1997). FGF-8 is associated with anteroposterior patterning and limb regeneration in *Xenopus*. *Dev. Biol.* **192**, 455–466.
- Cox, W. G. and Hemmati-Brivanlou, A. (1995). Caudalization of neural fate by tissue recombination and bFGF. *Development* **121**, 4349–4358.
- Darken, R. S. and Wilson, P. A. (2001). Axis induction by wnt signaling: target promoter responsiveness regulates competence. *Dev. Biol.* **234**, 42–54.

- Dichmann, D. S. and Harland, R. M.** (2012). fus/TLS orchestrates splicing of developmental regulators during gastrulation. *Genes Dev.* **26**, 1351–1363.
- Domigos, P. M., Itasaki, N., Jones, C. M., Mercurio, S., Sargent, M. G., Smith, J. C. and Krumlauf, R.** (2001). The Wnt/beta-catenin pathway posteriorizes neural tissue in Xenopus by an indirect mechanism requiring FGF signalling. *Dev. Biol.* **239**, 148–160.
- Durston, A. J., Timmermans, J. P. M., Hage, W. J., Hendriks, H. F. J., de Vries, N. J., Heideveld, M. and Nieuwkoop, P. D.** (1989). Retinoic acid causes an anteroposterior transformation in the developing central nervous system. *Nature* **340**, 140–144.
- Elkouby, Y. M., Elias, S., Casey, E. S., Blythe, S. A., Tsabar, N., Klein, P. S., Root, H., Liu, K. J. and Frank, D.** (2010). Mesodermal Wnt signalling organizes the neural plate via Meis3. *Development* **137**, 1531–1541.
- Elkouby, Y. M., Polevoy, H., Gutkovich, Y. E., Michaelov, A. and Frank, D.** (2012). A hindbrain-repressive Wnt3a/Meis3/Tsh1 circuit promotes neuronal differentiation and coordinates tissue maturation. *Development* **139**, 1487–1497.
- Elul, T., Koehl, M. A. R. and Keller, R.** (1997). Cellular mechanism underlying neural convergent extension in *Xenopus laevis* embryos. *Dev. Biol.* **191**, 243–258.
- Erter, C. E., Wilm, T. P., Basler, N., Wright, C. V. and Solnica-Krezel, L.** (2001). Wnt8 is required in lateral mesendodermal precursors for neural posteriorization in vivo. *Development* **128**, 3571–3583.
- Eyal-Giladi, H.** (1954). Dynamic aspects of neural induction in amphibia. *Arch. Biol. (Liege)* **65**, 179–259.
- Faas, L. and Isaacs, H. V.** (2009). Overlapping functions of Cdx1, Cdx2, and Cdx4 in the development of the amphibian *Xenopus tropicalis*. *Dev. Dyn.* **238**, 835–852.
- Fletcher, R. B., Baker, J. C. and Harland, R. M.** (2006). FGF8 spliceforms mediate early mesoderm and posterior neural tissue formation in *Xenopus*. *Development* **133**, 1703–1714.
- Frank, D. and Harland, R. M.** (1992). Localized expression of a *Xenopus* POU gene depends on cell-autonomous transcriptional activation and induction-dependent inactivation. *Development* **115**, 439–448.
- Frankenberg, S., Pask, A. and Renfree, M. B.** (2010). The evolution of class V POU domain transcription factors in vertebrates and their characterisation in a marsupial. *Dev. Biol.* **337**, 162–170.
- Garnett, A. T., Square, T. A. and Medeiros, D. M.** (2012). BMP, Wnt and FGF signals are integrated through evolutionarily conserved enhancers to achieve robust expression of Pax3 and Zic genes at the zebrafish neural plate border. *Development* **139**, 4220–4231.
- Gaunt, S. J., Cockley, A. and Drage, D.** (2004). Additional enhancer copies, with intact cdx binding sites, anteriorize Hoxa-7/lacZ expression in mouse embryos: evidence in keeping with an instructional cdx gradient. *Int. J. Dev. Biol.* **48**, 613–622.
- Gaunt, S. J., Drage, D. and Trubshaw, R. C.** (2008). Increased Cdx protein dose effects upon axial patterning in transgenic lines of mice. *Development* **135**, 2511–2520.
- Gilchrist, M. J., Zorn, A. M., Voigt, J., Smith, J. C., Papalopulu, N. and Amaya, E.** (2004). Defining a large set of full-length clones from a *Xenopus tropicalis* EST project. *Dev. Biol.* **271**, 498–516.
- Harland, R. M.** (1991). In situ hybridization: an improved whole-mount method for *Xenopus* embryos. *Methods Cell Biol.* **36**, 685–695.
- Heasman, J., Kofron, M. and Wylie, C.** (2000). Beta-catenin signalling activity dissected in the early *Xenopus* embryo: a novel antisense approach. *Dev. Biol.* **222**, 124–134.
- Hemmati-Brivanlou, A. and Melton, D. A.** (1994). Inhibition of activin receptor signalling promotes neuralization in *Xenopus*. *Cell* **77**, 273–281.
- Hemmati-Brivanlou, A., Kelly, O. G. and Melton, D. A.** (1994). follistatin, an antagonist of activin, is expressed in the Spemann organizer and displays direct neuralizing activity. *Cell* **77**, 283–295.
- Hollemann, T., Schuh, R., Pieler, T. and Stick, R.** (1996). *Xenopus* Xsal-1, a vertebrate homolog of the region specific homeotic gene spalt of *Drosophila*. *Mech. Dev.* **55**, 19–32.
- Isaacs, H. V., Pownall, M. E. and Slack, J. M.** (1998). Regulation of Hox gene expression and posterior development by the *Xenopus* caudal homologue Xcad3. *EMBO J.* **17**, 3413–3427.
- Itoh, K. and Sokol, S. Y.** (1997). Graded amounts of *Xenopus* dishevelled specify discrete anteroposterior cell fates in prospective ectoderm. *Mech. Dev.* **61**, 113–125.
- Kao, K. R. and Elinson, R. P.** (1985). Alteration of the anterior-posterior embryonic axis: the pattern of gastrulation in macrocephalic frog embryos. *Dev. Biol.* **107**, 239–251.
- Kengaku, M. and Okamoto, H.** (1995). bFGF as a possible morphogen for the anteroposterior axis of the central nervous system in *Xenopus*. *Development* **121**, 3121–3130.
- Khokha, M. K., Yeh, J., Grammer, T. C. and Harland, R. M.** (2005). Depletion of three BMP antagonists from Spemann's organizer leads to a catastrophic loss of dorsal structures. *Dev. Cell* **8**, 401–411.
- Kiecker, C. and Niehrs, C.** (2001). A morphogen gradient of Wnt/beta-catenin signalling regulates anteroposterior neural patterning in *Xenopus*. *Development* **128**, 4189–4201.
- Kiefer, S. M., McDill, B. W., Yang, J. and Rauchman, M.** (2002). Murine Sall1 represses transcription by recruiting a histone deacetylase complex. *J. Biol. Chem.* **277**, 14869–14876.
- Kohlhase, J., Wischerhoff, A., Reichenbach, H., Froster, U. and Engel, W.** (1998). Mutations in the SALL1 putative transcription factor gene cause Townes-Brocks syndrome. *Nat. Genet.* **18**, 81–83.
- Kohlhase, J., Heinrich, M., Schubert, L., Liebers, M., Kispert, A., Laccone, F., Turnpenny, P., Winter, R. M. and Reardon, W.** (2002). Okihiko syndrome is caused by SALL4 mutations. *Hum. Mol. Genet.* **11**, 2979–2987.
- Kolm, P. J., Apekin, V. and Sive, H.** (1997). *Xenopus* hindbrain patterning requires retinoid signaling. *Dev. Biol.* **192**, 1–16.
- Lamb, T. M. and Harland, R. M.** (1985). Fibroblast growth factor is a direct neural inducer, which combined with noggin generates anterior-posterior neural pattern. *Development* **121**, 3627–3636.
- Lamb, T. M., Knecht, A. K., Smith, W. C., Stachel, S. E., Economides, A. N., Stahl, N., Yancopoulos, G. D. and Harland, R. M.** (1993). Neural induction by the secreted polypeptide noggin. *Science* **262**, 713–718.
- Langmead, B., Trapnell, C., Pop, M. and Salzberg, S. L.** (2009). Ultrafast and memory-efficient alignment of short DNA sequences to the human genome. *Genome Biol.* **10**, R25.
- Lauberth, S. M. and Rauchman, M.** (2006). A conserved 12-amino acid motif in Sall1 recruits the nucleosome remodeling and deacetylase corepressor complex. *J. Biol. Chem.* **281**, 23922–23931.
- Lauberth, S. M., Bilyeu, A. C., Firulli, B. A., Kroll, K. L. and Rauchman, M.** (2007). A phosphomimetic mutation in the Sall1 repression motif disrupts recruitment of the nucleosome remodeling and deacetylase complex and repression of Gbx2. *J. Biol. Chem.* **282**, 34858–34868.
- Li, B., Kuriyama, S., Moreno, M. and Mayor, R.** (2009). The posteriorizing gene Gbx2 is a direct target of Wnt signalling and the earliest factor in neural crest induction. *Development* **136**, 3267–3278.
- Lim, C. Y., Tam, W.-L., Zhang, J., Ang, H. S., Jia, H., Lipovich, L., Ng, H.-H., Wei, C.-L., Sung, W. K., Robson, P. et al.** (2008). Sall4 regulates distinct transcription circuitries in different blastocyst-derived stem cell lineages. *Cell Stem Cell* **3**, 543–554.
- Livigni, A., Peradziriny, H., Sharov, A. A., Chia, G., Hammachi, F., Migueles, R. P., Sukparangsi, W., Pernagallo, S., Bradley, M., Nichols, J. et al.** (2013). A conserved Oct4/POUV-dependent network links adhesion and migration to progenitor maintenance. *Curr. Biol.* **23**, 2233–2244.
- Lu, J., Jeong, H. W., Kong, N., Yang, Y., Carroll, J., Luo, H. R., Silberstein, L. E. and Yupoma, L.** (2009). Stem cell factor SALL4 represses the transcriptions of PTEN and SALL1 through an epigenetic repressor complex. *PLoS ONE* **4**, e5577.
- McGrew, L. L., Lai, C.-J. and Moon, R. T.** (1995). Specification of the anteroposterior neural axis through synergistic interaction of the Wnt signalling cascade with noggin and follistatin. *Dev. Biol.* **172**, 337–342.
- McKendry, R., Hsu, S.-C., Harland, R. M. and Grosschedl, R.** (1997). LEF-1/TCF proteins mediate wnt-inducible transcription from the *Xenopus* nodal-related 3 promoter. *Dev. Biol.* **192**, 420–431.
- Monsoro-Burq, A.-H., Wang, E. and Harland, R.** (2005). Msx1 and Pax3 cooperate to mediate FGF8 and WNT signals during *Xenopus* neural crest induction. *Dev. Cell* **8**, 167–178.
- Morrison, G. M. and Brickman, J. M.** (2006). Conserved roles for Oct4 homologues in maintaining multipotency during early vertebrate development. *Development* **133**, 2011–2022.
- Neff, A. W., King, M. W. and Mescher, A. L.** (2011). Dedifferentiation and the role of sall4 in reprogramming and patterning during amphibian limb regeneration. *Dev. Dyn.* **240**, 979–989.
- Nicetto, D., Hahn, M., Jung, J., Schneider, T. D., Straub, T., David, R., Schotta, G. and Rupp, R. A. W.** (2013). Suv4-20h histone methyltransferases promote neuroectodermal differentiation by silencing the pluripotency-associated Oct-25 gene. *PLoS Genet.* **9**, e1003188.
- Nieuwkoop, P. D.** (1952). Activation and organization of the central nervous system in amphibia. Part III. Synthesis of a new working hypothesis. *J. Exp. Zool.* **120**, 83–108.
- Nieuwkoop, P. D. and Faber, J.** (1967). *Normal Table of Xenopus Laevis* (Daudin). New York: Garland Publishing.
- Nieuwkoop, P. D., Boterenbrood, E. C., Kremer, A., Bloemsma, F. F. S. N., Hoessels, E. L. M. J., Meyer, G. and Verheyen, F. J.** (1952a). Activation and organization of the central nervous system in amphibia. Part I. Induction and activation. *J. Exp. Zool.* **120**, 1–31.
- Nieuwkoop, P. D., Boterenbrood, E. C., Kremer, A., Bloemsma, F. F., Hoessels, E. L. M. J., Meyer, G. and Verheyen, F. J.** (1952b). Activation and organization of the central nervous system in amphibia. Part II. Differentiation and organization. *J. Exp. Zool.* **120**, 33–81.
- Obrig, T. G., Culp, W. J., McKeehan, W. L. and Hardesty, B.** (1971). The mechanism by which cycloheximide and related glutarimide antibiotics inhibit peptide synthesis on reticulocyte ribosomes. *J. Biol. Chem.* **246**, 174–181.
- Onai, T., Sasai, N., Matsui, M. and Sasai, Y.** (2004). *Xenopus* Xsalf: anterior neuroectodermal specification by attenuating cellular responsiveness to Wnt signalling. *Dev. Cell* **7**, 95–106.

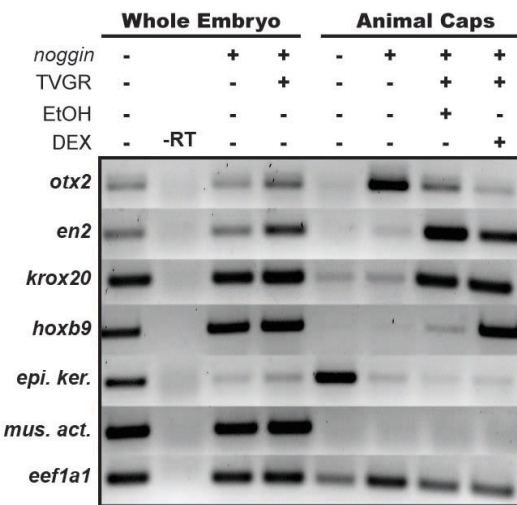
- Onuma, Y., Nishinakamura, R., Takahashi, S., Yokota, T. and Asashima, M.** (1999). Molecular cloning of a novel *Xenopus* spalt gene (*Xsal-3*). *Biochem. Biophys. Res. Commun.* **264**, 151-156.
- Pilon, N., Oh, K., Sylvestre, J.-R., Bouchard, N., Savory, J. and Lohnes, D.** (2006). Cdx4 is a direct target of the canonical Wnt pathway. *Dev. Biol.* **289**, 55-63.
- Pilon, N., Oh, K., Sylvestre, J.-R., Savory, J. G. A. and Lohnes, D.** (2007). Wnt signaling is a key mediator of Cdx1 expression in vivo. *Development* **134**, 2315-2323.
- Prinos, P., Joseph, S., Oh, K., Meyer, B. I., Gruss, P. and Lohnes, D.** (2001). Multiple pathways governing Cdx1 expression during murine development. *Dev. Biol.* **239**, 257-269.
- Ribisi, S., Mariani, F. V., Aamar, E., Lamb, T. M., Frank, D. and Harland, R. M.** (2000). Ras-mediated FGF signaling is required for the formation of posterior but not anterior neural tissue in *Xenopus laevis*. *Dev. Biol.* **227**, 183-196.
- Rousse, S. Z., Ben-Haroush Schyr, R., Gur, M., Zouela, N., Kot-Leibovich, H., Shabtai, Y., Koutsi-Urschanski, N., Baldessari, D., Pillemer, G., Niehrs, C. et al.** (2011). Negative autoregulation of Oct3/4 through Cdx1 promotes the onset of gastrulation. *Dev. Dyn.* **240**, 796-807.
- Ruiz i Altaba, A. and Jessell, T. M.** (1991). Retinoic acid modifies the pattern of cell differentiation in the central nervous system of neurula stage *Xenopus* embryos. *Development* **112**, 945-958.
- Sakaki-Yumoto, M., Kobayashi, C., Sato, A., Fujimura, S., Matsumoto, Y., Takasato, M., Kodama, T., Aburatani, H., Asashima, M., Yoshida, N. et al.** (2006). The murine homolog of SALL4, a causative gene in Okihiro syndrome, is essential for embryonic stem cell proliferation, and cooperates with Sall1 in anorectal, heart, brain and kidney development. *Development* **133**, 3005-3013.
- Sasaki, Y., Lu, B., Steinbeisser, H., Geissert, D., Gont, L. K. and De Robertis, E. M.** (1994). Xenopus chordin: a novel dorsalizing factor activated by organizer-specific homeobox genes. *Cell* **79**, 779-790.
- Shiotsugu, J., Katsuyama, Y., Arima, K., Baxter, A., Koide, T., Song, J., Chandraratna, R. A. S. and Blumberg, B.** (2004). Multiple points of interaction between retinoic acid and FGF signaling during embryonic axis formation. *Development* **131**, 2653-2667.
- Simeone, A.** (2000). Positioning the isthmic organizer where Otx2 and Gbx2 meet. *Trends Genet.* **16**, 237-240.
- Sive, H. L., Draper, B. W., Harland, R. M. and Weintraub, H.** (1990). Identification of a retinoic acid-sensitive period during primary axis formation in *Xenopus laevis*. *Genes Dev.* **4**, 932-942.
- Sive, H. L., Grainger, R. M. and Harland, R. M.** (2010). *Early Development of Xenopus Laevis*. Cold Spring Harbor, NY: Cold Spring Harbor Laboratory Press.
- Snir, M., Ofir, R., Elias, S. and Frank, D.** (2006). Xenopus laevis POU91 protein, an Oct3/4 homologue, regulates competence transitions from mesoderm to neural cell fates. *EMBO J.* **25**, 3664-3674.
- Sweetman, D. and Münsterberg, A.** (2006). The vertebrate spalt genes in development and disease. *Dev. Biol.* **293**, 285-293.
- Takemoto, T., Uchikawa, M., Kamachi, Y. and Kondoh, H.** (2006). Convergence of Wnt and FGF signals in the genesis of posterior neural plate through activation of the Sox2 enhancer N-1. *Development* **133**, 297-306.
- Trapnell, C., Pachter, L. and Salzberg, S. L.** (2009). TopHat: discovering splice junctions with RNA-Seq. *Bioinformatics* **25**, 1105-1111.
- Trapnell, C., Williams, B. A., Pertea, G., Mortazavi, A., Kwan, G., van Baren, M. J., Salzberg, S. L., Wold, B. J. and Pachter, L.** (2010). Transcript assembly and quantification by RNA-Seq reveals unannotated transcripts and isoform switching during cell differentiation. *Nat. Biotechnol.* **28**, 511-515.
- Tsukamoto, N., Ichisaka, T., Okita, K., Takahashi, K., Nakagawa, M. and Yamanaka, S.** (2009). Roles of Sall4 in the generation of pluripotent stem cells from blastocysts and fibroblasts. *Genes Cells* **14**, 683-694.
- Uchikawa, M., Ishida, Y., Takemoto, T., Kamachi, Y. and Kondoh, H.** (2003). Functional analysis of chicken Sox2 enhancers highlights an array of diverse regulatory elements that are conserved in mammals. *Dev. Cell* **4**, 509-519.
- van den Akker, E., Forlani, S., Chawengsaksophak, K., de Graaff, W., Beck, F., Meyer, B. I. and Deschamps, J.** (2002). Cdx1 and Cdx2 have overlapping functions in anteroposterior patterning and posterior axis elongation. *Development* **129**, 2181-2193.
- van de Ven, C., Bialecka, M., Neijts, R., Young, T., Rowland, J. E., Stringer, E. J., van Rooijen, C., Meijlink, F., Növoa, A., Freund, J.-N. et al.** (2011). Concerted involvement of Cdx/Hox genes and Wnt signaling in morphogenesis of the caudal neural tube and cloacal derivatives from the posterior growth zone. *Development* **138**, 3451-3462.
- Wang, W. C. H. and Shashikant, C. S.** (2007). Evidence for positive and negative regulation of the mouse Cdx2 gene. *J. Exp. Zool. B Mol. Dev. Evol.* **308B**, 308-321.
- Wu, Q., Chen, X., Zhang, J., Loh, Y.-H., Low, T.-Y., Zhang, W., Zhang, W., Sze, S.-K., Lim, B. and Ng, H.-H.** (2006). Sall4 interacts with Nanog and co-occupies Nanog genomic sites in embryonic stem cells. *J. Biol. Chem.* **281**, 24090-24094.
- Yang, J., Chai, L., Liu, F., Fink, L. M., Lin, P., Silberstein, L. E., Amin, H. M., Ward, D. C. and Ma, Y.** (2007). Bmi-1 is a target gene for SALL4 in hematopoietic and leukemic cells. *Proc. Natl. Acad. Sci. U.S.A.* **104**, 10494-10499.
- Yang, J., Corsello, T. R. and Ma, Y.** (2012). Stem cell gene SALL4 suppresses transcription through recruitment of DNA methyltransferases. *J. Biol. Chem.* **287**, 1996-2005.
- Yost, C., Torres, M., Miller, J. R., Huang, E., Kimelman, D. and Moon, R. T.** (1996). The axis-inducing activity, stability, and subcellular distribution of beta-catenin is regulated in *Xenopus* embryos by glycogen synthase kinase 3. *Genes Dev.* **10**, 1443-1454.
- Zhang, J., Tam, W.-L., Tong, G. Q., Wu, Q., Chan, H.-Y., Soh, B.-S., Lou, Y., Yang, J., Ma, Y., Chai, L. et al.** (2006). Sall4 modulates embryonic stem cell pluripotency and early embryonic development by the transcriptional regulation of Pou5f1. *Nat. Cell Biol.* **8**, 1114-1123.

## Supplementary Material

**A**



**B**



**C**

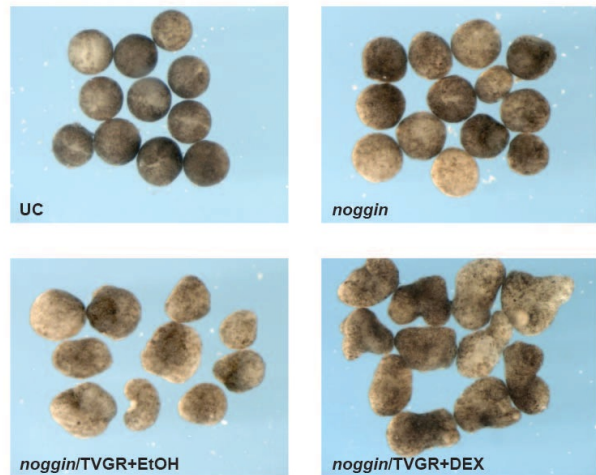


**Figure S1: TVGR activates canonical Wnt signaling.** (A) Quantification of secondary axis induction by ventral vegetal injection of TVGR at the 4-cell stage with representative tadpoles from each class. (B) RT-PCR on 5 whole embryos or 25 animal caps treated with the indicated reagents. -RT: reaction done in the absence of Reverse Transcriptase, *epi. ker.*: epidermal keratin (epidermis), *mus. act.*: muscle actin (mesoderm) (C) Animal caps treated with the indicated reagents.

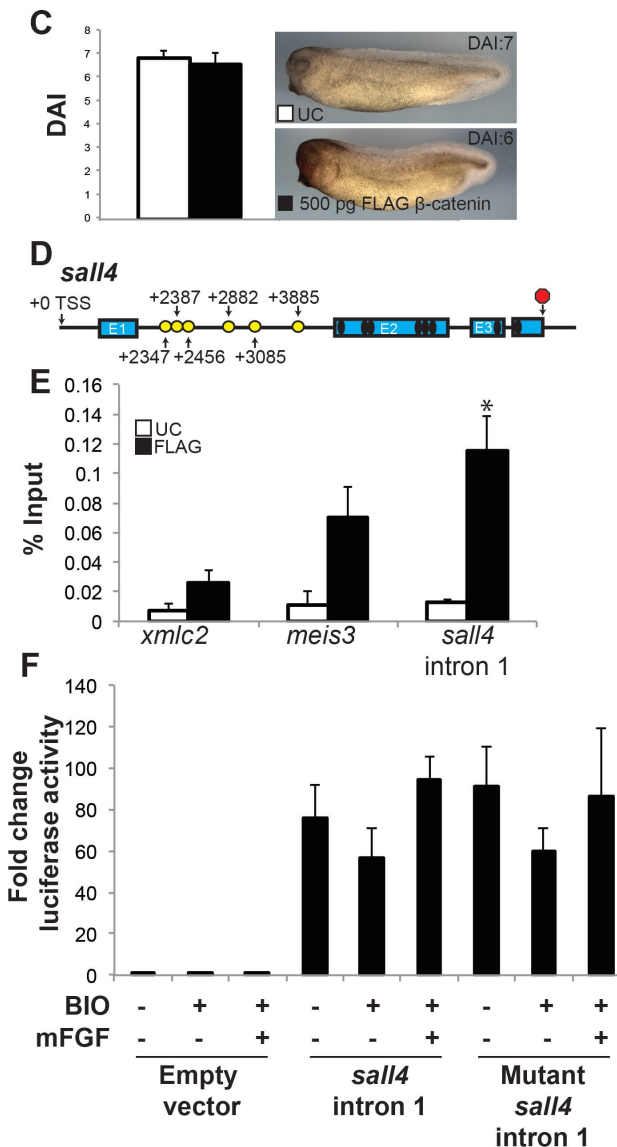
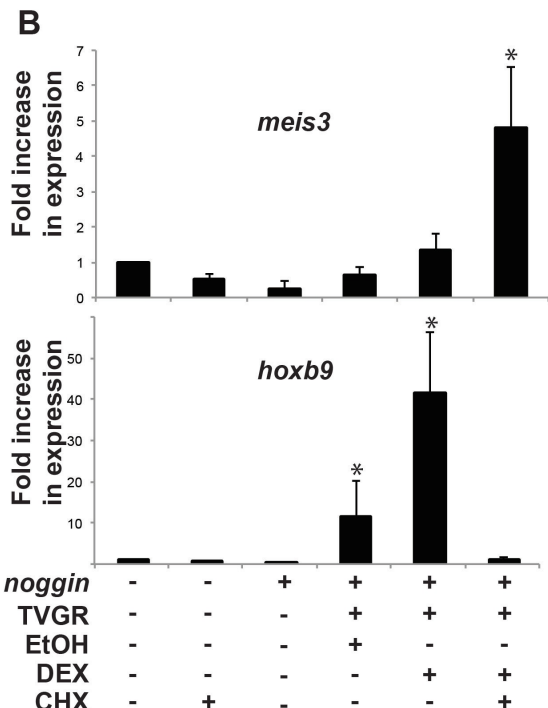
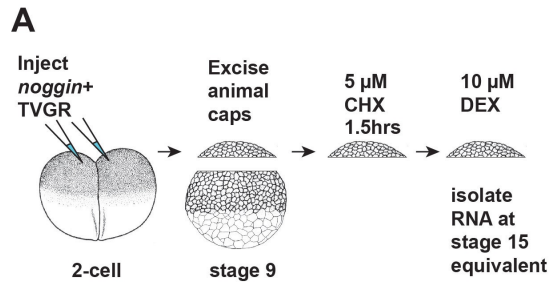


**Figure S2: Intron 1 of *sall4* binds β-catenin but does not mediate a Wnt signal.** (A) Using animal caps to screen for direct transcriptional targets of Wnt in neural tissue. (B) qPCR on 15-25 animal caps treated as indicated on the X-axis. The Y-axis shows expression relative to *odc*, *meis3* and *hoxb9* serve as controls for known direct and indirect targets of Wnt, respectively. (C) Quantification of dorsalization in uninjected embryos (open bars) and embryos injected animally with 500 pg FLAG-tagged β-catenin RNA (250 pg/blastomere) at the 2-cell stage (filled bars) as scored by the dorsoanterior index (DAI). Error bars: 1 SEM. Images show a representative uninjected (UC) embryo with a DAI of 7 (normal) and a representative embryo with a DAI of 6 (kinked axis). (D) Schematic of the genomic locus of *sall4* in *Xenopus laevis* (Xenbase.org). Blue boxes indicate exons and yellow circles indicate the location of putative TCF/LEF binding sites. Black ovals show the locations of the zinc-finger domains. Numbers indicate the position of putative binding sites relative to the transcription start site (TSS). (E) Chromatin immunoprecipitation of FLAG-tagged β-catenin in late gastrulae/early neurulae. Open bars represent uninjected embryos and closed bars represent embryos injected with 500 pg FLAG-tagged β-catenin (250 pg/blastomere at the 2-cell stage). Error bars: 1 SEM per cent input for each measurement. (F) Luciferase reporter assays in HEK293 cells treated with or without BIO and/or mouse FGF. Error bars: 1 SEM. All means were compared by one-way ANOVA followed by Tukey post-hoc analyses (\*: p<0.05).

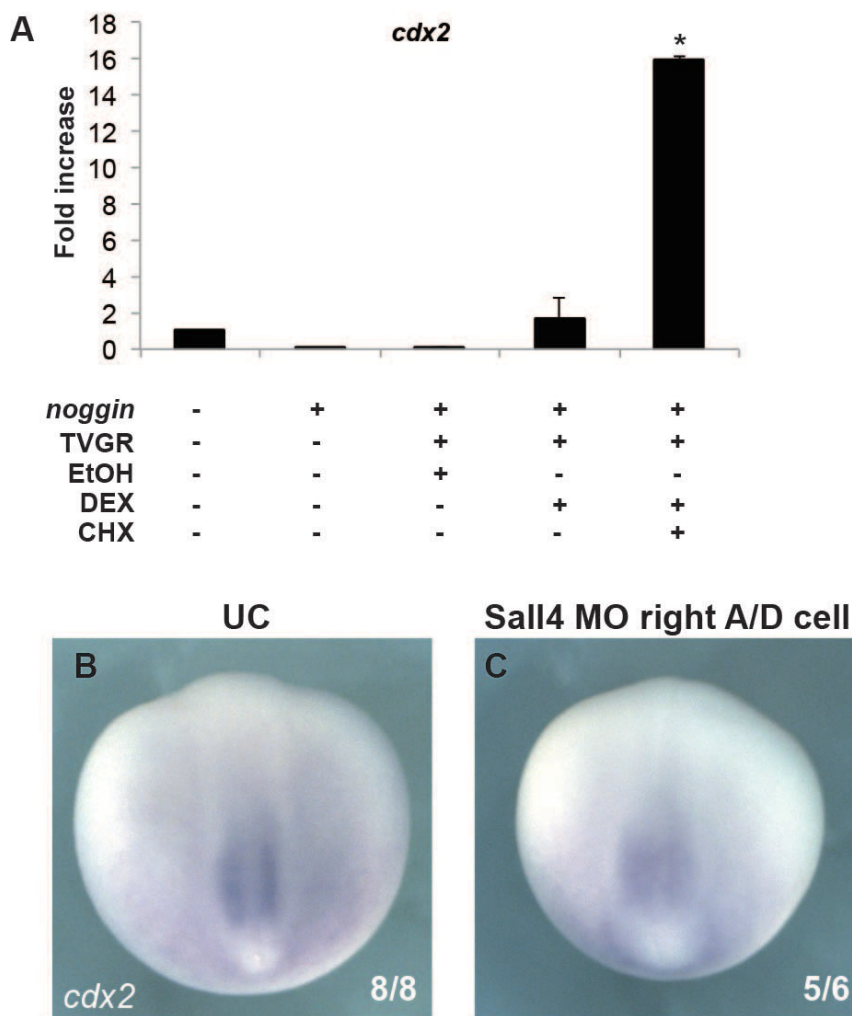


**Figure S3: *cdx2* is activated by canonical Wnt signaling and not affected by Sall4 knockdown** (A) qPCR on 5 whole embryos or 15 to 25 animal caps treated according to the conditions indicated on the X-axis. The Y-axis shows expression relative to *odc*. Error bars: 1 SEM. (B-C) *cdx2* expression at stage 18. Dorsal views with the anterior oriented towards the top. (B) Uninjected control embryo. (C) Embryo injected with 20 ng Sall4 MO in one animal-dorsal cell at the 4-cell stage.

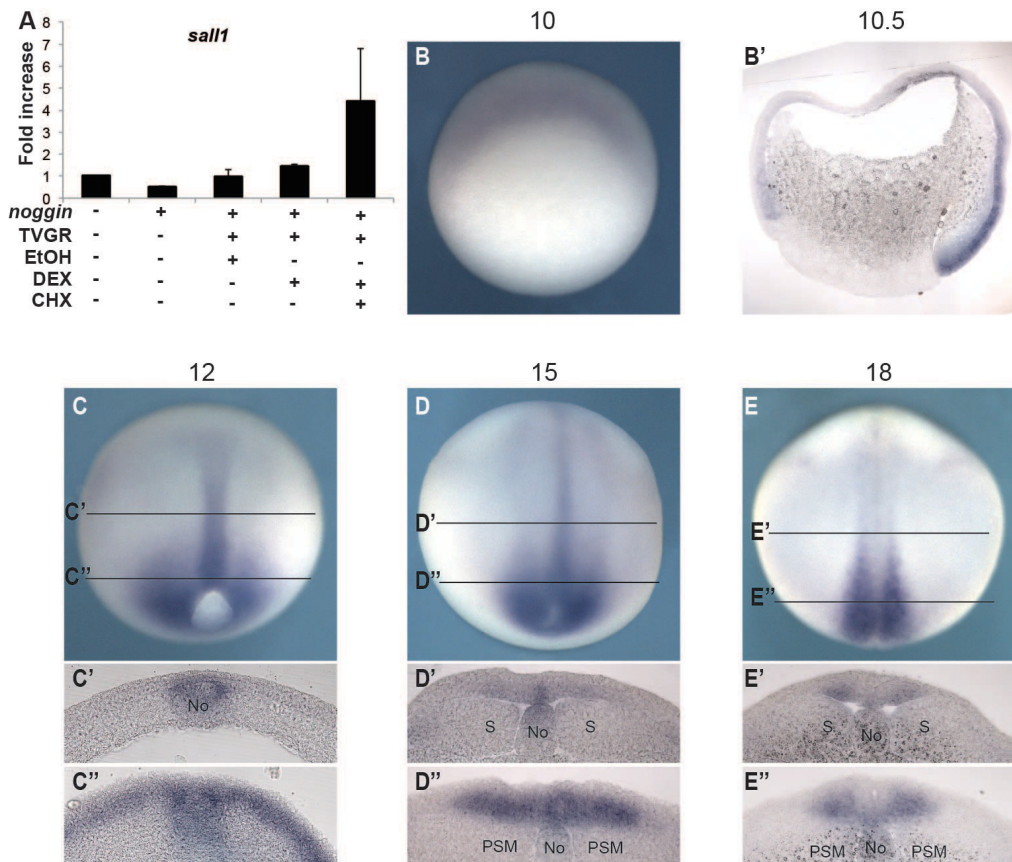
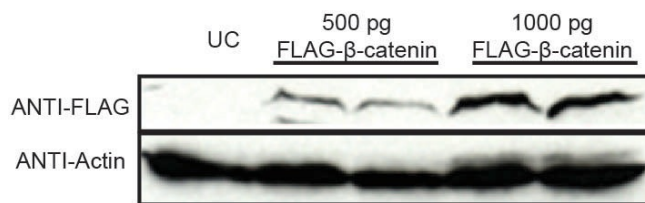


**Figure S4: *sall1* is activated by canonical Wnt signaling and expressed during early embryogenesis.** (A) qPCR on 5 whole embryos or 15 to 25 animal caps treated according to the conditions indicated on the X-axis. The Y-axis shows expression relative to *odc*. Error bars: 1 SEM. (B-E) Whole-mount *in situ* hybridizations of *sall1* in *Xenopus laevis* embryos. (B) Whole mount stage 10 embryo stained for *sall1*, dorso-vegetal view with the dorsal lip of the blastopore oriented towards the top. (B') Sagittal section of stage 10.5 embryo stained for *sall1* expression, animal pole is to the top and dorsal is to the right. (C-D) Dorsal views of indicated neurula stage embryos, anterior is oriented towards the top. (C'-C'') Transverse sections of stage 12 embryos stained for *sall1*, (C') anterior and (C'') posterior. (D'-D'') Transverse sections of stage 15 embryos stained for *sall1*, (D') anterior and (D'') posterior. (E'-E'') Transverse sections of stage 18 embryos stained for *sall1*, (E') anterior and (E'') posterior. (B', C'-E'') 50  $\mu$ M sections, (C'-E'') dorsal oriented towards the top. No: notochord, S: somite, PSM: presomitic mesoderm.

**A**



**B**

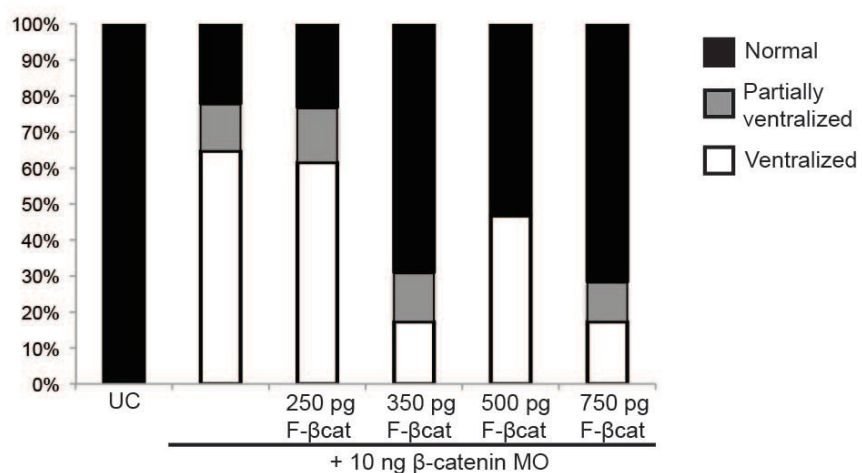


**Figure S5: Injected embryos express functional FLAG-tagged β-catenin. (A)** Western blot for the FLAG epitope in injected embryos. Actin serves as the loading control. **(B)** Ventralization of embryos injected with β-catenin MO and co-injection with FLAG-tagged β-catenin RNA. F-βcat: FLAG-tagged β-catenin.

**Figure S6: Sequence of *sall4* intron 1 in *Xenopus laevis*.** Sequence from *X. laevis* genome ([xenbase.org](http://xenbase.org)) coordinates: Scaffold1115:232,200..237,499. Putative TCF/LEF binding sites are indicated in red. Priming sites used for ChIP-qPCR are highlighted in yellow. Underlined sequences show TCF/LEF sites tested in ChIP.

GAGTCGCACTTGCTCTGGCTGCCTTATAGAGCGCAAGTGGCATTAAACCGAGAGGAGCGTGGCTGC  
 TGCGCTCCATTCCCTCCGAGCTGCCCACCGCCAAGGTGATCGAATACAGGGCTGGATTGTCTCCCTCTCA  
 GTCTGCAGCGCTCTCCTTACATACAGCTGCTCTCGTGCACCTTCCCCTCTATTACCTTTCTATT  
 ATTATTATTATTATTGATTATTATAATAGTATTATTATTAAATTGTAGCAATTCCAGGGTATATTGACCCC  
 ACCTGTGGGCTTATGGATCCATGTGATTGGAAGCACCTGTGGCTGTAATCATATATT  
 TTTTTTTTTTTTTAATACCCTGGTAGTGTGCTGCTTATTCTAGTGTATAATTAAAGCAAAGAAAGGAAG  
 AAAACAGGGGTGACTAGTTAGTCACCCCTCAACCCCTCCCTCACACCCCCACCCCTCCATCCTCAT  
 CCTCTCTTCTCTAAGGCATTCCAATCTGATTCCCCACTCCAAAATATCCTCCCTGTGCTCCTGGGTC  
 AGAGGGAACCAGCAGAAGCAGCACCTGTGTCTGTGCTTGGTAGGTTAATTATCCTCATATAT  
 TCTAGGGACTGGGTTAATGTGTTGTACCTGCTTAAATTCCGTTATCGAAATAGCAGAAGGGGTACACA  
 AAGTTTTATGTAGTATCTGTATATTCTGTTATCTATTAAATCTATTTATATTGTGTTATTCATAAT  
 CTCAATGAGGGGCACAGTCCTGCCATTACATTCTATTCATCTGCATNNNNNNNNNNNNNNNNNNNNNN  
 NNN  
 TCCACCTTAGTCCAAATCTAATTAGCAATTCTATGCACTCCCTCCCTTATTCCCTTATTACAATGCAA  
 TTTTATTCTGTTGTCTGGAACATACTGGTACTAATTAACAATCCAGGAAACCAGCAGGTGGGGAGTGG  
**AAGG**TACAAAGCTACATATTGAAATTATCATATGAACAAAGAGGTGCCAATGCCTGTGTTATCATCAGATA  
 CTGGGATTGCCCTGTTAATCTCAAGGTTAATCTTTCAAAGACTTCCATTAGTGTACTAGACCATTAA  
 ATATATTATTTCGTCTATTGTTGGTTATAGAGTCTGATCTGGCAACTCTCAATTAAATAACTGATAAA  
 CAGAAGAGCTACAGATGTAAGAATTGAAATCCGAAAGCATTCTCAAATGAATGTATGGTACAGTAGA  
 GTGTTTTGGGGGGGCATGTTGGTTGTGTAGGTGAAACATAGGGCAACAGTTGAATAGTAGGTGCT  
 AGGACAAAATGGCATTGTCACCTTGTGAAGTTCAAGACCCTAGAACCTTGACAGGCCAAGCATGGAGT  
 TGCACTTAAACAGATGAAGGTTGAACAGTCTAGTCTAAATGGCTGCAATAATGGGCCTGCAATATCTATTCT  
 TCCCCCTCAGAGTCCTTACTAACAAAGCCCTGGTATAGATCTGCAAATGGAACATTGCATATCCCCCTAACTT  
 TACTTTTTCTTTAACTGGAAAAAAATGCTCGTTGTGACCTTGTGACGCTGAGTGTAGTGCT  
 AAGTACAGGCATAAACATAAACTATTATTCATTAAGTGGTCTGCAACAAAACATAATTCCCTGGCTGGCTG  
 TTAACAAAGCTAATTCACTCACAGCAGGGTCGGGCTGTCAGTAAGGTACTTGGGCCAGATGGCTGCAAAC  
 GCAATCAGGAACCTGCTGGTGTGAGTGCACCTCTATTAAACACACTTAAACAAAT

TATTTAAATGAGATAAATCTATCTCTATATCTAAAGAGAAATCACACCACTTTGAAGATTTTT  
TATAATCTACTATTCACCCCTACTTTCTGGTTTTATTATGAGTGTCTAGAGGTTATGTAATGATTC  
ATCACTGGGCATATAACACGTGGAGGAGGCTCCTTAACCTGGTGGGTTTCTTAGCTAAGGGTCAGTG  
TTGGATGCGGCAGACTAGGTTAACACACAGCCTATCTGTTACAGGTGAAGGGTAAACGAGGCCAACTGG  
TTTGTAGTTGCTCTTGTACAGTGTAAAGGTGCCGGTGGCCTGCTGGTATAACCTCTGGCTCCTAGTGTGG  
GTGGCAGGTTAATGTCAGGACTGATCCCAGTAGGGTTGTCCATTGCCAATTATGTGACTATTGGTGACCGATT  
TTGTTCACCTCCGATCTGTTGTGGAGACCAGAAAGATTCTGATGATTTCCTTAGTGGTTGTCTTTAGAG  
GCAGTTTGCTTCAGTAAAAATATTCTGCTCAATGTGAAATTGCACTGACAATGAGGAATAGATATGGC  
GGGCAGGCAGCTTGAGTCAGTCAAGTGGGTCCACATAATTTCATTAATTAAA**ATGTTTC**CATA  
CCTCCAATGCTGCCTTGCCTGGTCAGGGAAAGGATTGTATAGAATATATGCCAGCTTAATGGCTGTACAGA  
AGTTGGTCAGCATACAGGGATGTTCATCTGTGCTGCTGAATAAGATCCGTTTGGGTTACTTTCTGTAG  
TCCCTCAGTGATTTGTAAATCCACGTGAGTATTACCATACATGTGCTGAGCACTAACACAGGATGAGT  
GAATCAGAAAAGGAACGTGACTGTAGCTGTAAATAGATGGCCTCAAGCATTGCTCTGGGAGATGGGGTAAGTG  
ATCGGCCGCTTCATTTAGAGCAGGGATGATCGGTGCTCACTAAACCAAATCTCCCACCAGCAATGGCT  
GAGAGTTACCCAACATTAAAGTGCAGGCTCACATATTGACAACTTGAGTTAGGTGTCAAGTGAACCTC  
CTGCTAGAATAAATTATTTTTAGAGGGAGAATTAATATTACCTGCAAAGGGTCTGTATAATATTACA  
TTTGCATAATTGGCACGGAAAGGCTCTCAATCACTTTAACACATCAACATAACTGACAATAGGCTTGCATCTC  
CCCTCCCCAATCCATTGTTAGTGATTTAACCTGCTGACTCATTGCTTAACATTGGA  
TAAATAGATGCTGAGATAACATTGAGATTGAGCAGTGGAGATGCACCCATGTACAGTATCCCCCTGCTCT  
TTGTTTTTTTTGTTTTATTAGCATTATTAAGATCCCTCACTGTTTATTAAATTTCATTGAAA  
TTACCAATTTCATCACTGAAACTACAGGAGATTGTTGATGAAATAAGTAGGTTTATTCAAGTTACT  
ACTGCTAGAACTATCAATGGATCTTACATTAGTACTTTAGGTAGAGTTATTGTTCTGCAGAGATGTCA  
GCAAAGAGCGTGTACTATTGAGAAACAAGAAAAATAAGAAATTGCATCCTGCCGTGGGACCTTAAG  
CGTTAACGCCGGTTATGCTCAGCTGTTGAAACCAGGCAACTTAAGATATTGCGACATAAAATC  
AGACTCCTTAAAGAGAGATGAATTAAAGCTAGCCATAGACGTGCAGATTAGACAAACGAACGTCTTCCAAT  
ACTCCTACCTGCAAATAACCATTGAGATTATTAAGTTGCAAAGAGAACAAATTGCACGATCGGGCCATT  
TTGACTGGCGGCAATGTTGAAAGTTATGTTGACAAACGGTAGTTACTGTCCTCCATTGATAGCTGTAGCCG  
ATCTAAATCTTAAACCTGTCGATTGACCGCGTGAAACGAAAAATGCTTAACATTCCACAGTTCTGAAAAT  
CGTACAAAATTTTGTGATCGTACTGTGTCTAGGGCGGCGATGCCGTGGGACATGATTGTTAGAATT  
GTTCCAGTACAATTGCCATAATTGCTATTCAAATGTGGTTGCTGCAATTGTCAGCTAATAAATTAGCTTT  
GTATCTCTAGCAATGGTGAATCTGTTGGGTAGGACCTGTAAGTTCTATTAAATTGGCCAAACAATCTGGT  
TAACTTTTTTTTTAACCTTTACAG

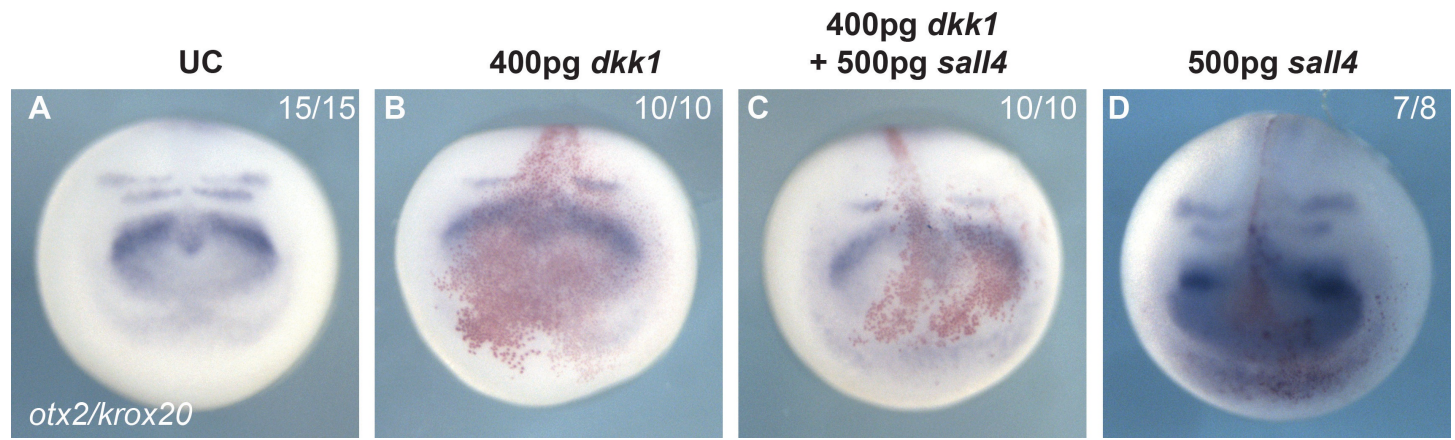


**Figure S7: Sall4 does not rescue Dkk1-induced anteriorization.** (A-D) Anterior views of whole-mount *in situ* hybridizations for *otx2* and *krox20* on *Xenopus laevis* embryos. (A) Uninjected control (UC). (B) Embryo injected with 400pg *dkk1* RNA. (C) Embryo injected with 400pg *dkk1* and 500pg *sall4* RNA. (D) Embryo injected with 500pg *sall4* RNA.

**Table S1: List of all primers used.** RT-PCR: Conventional RT-PCR. qPCR: quantitative PCR. WMISH: Used to make a probe for whole mount *in situ* hybridization. ChIP: Used for qPCR on immunoprecipitated chromatin.

Gene	Forward	Reverse
<i>cdx2</i> (qPCR)	5'-ACATACCGGGATCCAAGACA-3'	5'-CAGCCTGAGTCTGCTGGATT-3'
<i>eef1a1</i> (RT-PCR/qPCR)	5'-CCCTGCTGGAAGCTCTGAC-3'	5'-GGACACCAGTCTCACACGA-5'
<i>en2</i> (RT-PCR)	5'-CAGCCTGGGTCTACTGCAC-3'	5-CTTGCCCTCTGCTCAGT-3'
<i>epidermal keratin</i> (RT-PCR)	5'-GACCTGGAAGGGAAGATCC-3'	5'-GAAGAGGCCAGCTCATTCTCAA-3'
<i>hoxb9</i> (qPCR)	5'-TACTTACGGGCTTGGCTGGA-3'	5'-AGCGTGTAAACCAGTTGGCTG-3'
<i>hoxb9</i> (RT-PCR)	5'-CTCCAGCAGCAAATTCTCT-3'	5'-CAGTTGGCTGAGGGGTTG-3'
<i>krox20</i> (RT-PCR)	5'- CCAGTGACTTTGGTAGTTGTG-3' ,	5'-TGGACGAGTAGGAGAAATCCA-3'
<i>meis3</i> (ChIP)	5'- CACTGTAAGTTATTGCCTCAAAGG-3' ,	5'-AGCTTGTAAACTTGTGGGCTTT-3'
<i>meis3</i> (qPCR)	5'-CAGGATACAGGGCTCACGAT-3'	5'-CTTGGGGCTGCTGTGTAAATC-3'
<i>meis3</i> (RT-PCR)	5'-ATGATCGTGATGGCTCTTCC-3'	5'-CCCTGTGCGATTAGATTGGT-3'
<i>muscle actin</i> (RT-PCR)	5'-GACTCTGGGATGGTGTGAC-3'	5'-AGCAGTGGCCATTTCATTCT-3'
<i>odc</i> (RT-PCR/qPCR)	5'-GGGCTGGATCGTATCGTAGA-3'	5'-TGCCAGTGTGGCTTGACAT-3'
<i>otx2</i> (RT-PCR)	5'-TATCTCAAGCAACCGCCATA-3'	5'-AACCAAACCTGGACTCTGGA-3'
<i>pou25</i> (qPCR)	5'-GGGCCACCACTATCCCTAAT-3'	5'-GTGTGTAGCCCAGGGACACT-3'
<i>pou60</i> (qPCR)	5'-AGTTTGCCAAGGAGCTGAAA-3'	5'-GGACTCAAAGCGGCAGATAG-3'
<i>pou91</i> (qPCR)	5'-ACTTATTGCCCCGTCTCCT-3'	5'-CCCCATTCAAGATCACTTGCT-3'
<i>sall1</i> (qPCR)	5'-GAGAGGGTCAAATCCATCG-3'	5'-GGAGGTGGTGGATTTCATTC-3'
<i>sall1</i> (WMISH probe)	5'-CTTCAAAGCATGGTGAGCA-3'	5'-ATGGCACGATGGACACTGTA-3'
<i>sall4</i> (qPCR)	5'-TGTCAAAGGATGAGCATTG-3'	5'-CATGCGGTAGAGGGTACTT-3'
<i>sall4</i> (WMISH probe)	5'-CTTGGTGCGCACTTATCTCA-3'	5'-GCCTCAGATTGTGTGGACT-3'
<i>sall4</i> intron 1 (ChIP)	5'- GGGAGTTGGAAGGTACAAAGC-3' ,	5'-AACCAAACAATAGACGAAAAATAAA-3'
<i>xmle2</i> (ChIP)	5'- TGGGATATTTACTGAACACAATG-3'	5'-CGTCCTGTGCCACCTAATG-3'

<b>Gene</b>	<b>Forward</b>	<b>Reverse</b>
<b>WT <i>sall4</i> intron 1</b> (Luciferase assay)	5'-CACTCCCTCCCCTTATTCC-3'	5'-CACTCCCTCCCCTTATTCC-3'
<b><i>sall4</i> intron 1 TCF/LEF site +2347</b> (mutagenesis)	5'-GGAGTTGGAAGGTACGGG GCTACATATTG-3'	5'-CAATATGTAGCCCCGTACCTTC AACTCC-3'
<b><i>sall4</i> intron 1 TCF/LEF site +2387</b> (mutagenesis)	5'-CATATGAACGGGGAGGTC GCCAATG-3'	5'-CATTGGCGACCTCCCCGTTCATAT G-3'
<b><i>sall4</i> intron 1 TCF/LEF site +2465</b> (mutagenesis)	5'-GGTTAATCTTCGGGGACT TCCATTAGTG-3'	5'-CACTAAATGGAAGTCCCCGAAA GATTAACC-3'

**Table S2: Genes with >2-fold expression (direct Wnt activation vs. anterior neural) found by RNA-Seq.**

The data represents cold increase as measured by fragments per kilobase of exon per million reads (FPKM). The nature of this quantification can lead to high fold changes in lowly expressed genes and likely accounts for the massive fold increases calculated in genes with the highest differential expression.

<u>Gene</u>	<u>Clone ID</u>	<u>Fold Increase</u>
hnRNP H3	gi 52138902 gb BC082630.1	1.51235E+11
H3 histone, family 3B	gi 27503243 gb BC042290.1	1.03963E+11
Glutamate ammonia ligase	gi 49256010 gb BC073448.1	39422399227
Protein phosphatase type 1 alpha, catalytic subunit	gi 27695193 gb BC041730.1	2824225487
Ki-67	gi 115527315 gb BC124560.1	1131777.541
copper chaperone for superoxide dismutase	gi 50418348 gb BC077488.1	3919.698435
FoxI4.2	gi 50418055 gb BC078036.1	1329.542265
Ephrin-A4	gi 183985625 gb BC166129.1	1297.844383
smad4	gi 54037962 gb BC084196.1	1053.601949
Cdx-2	gi 84105446 gb BC111473.1	600.0062069
Eukaryotic translation initiation factor 3 subunit 10	gi 35505403 gb BC057711.1	414.3164277
Churchill	gi 114107852 gb BC123207.1	369.3076365
pip4k2a	gi 120537387 gb BC129059.1	328.1431677
hnRNPK	gi 27882468 gb BC044711.1	319.4817015
MGC83026	gi 49118646 gb BC073670.1	226.469437
tpno2	gi 54673692 gb BC084978.1	222.1449285
nol12	gi 114107789 gb BC123345.1	151.6234281
epithelial V-like antigen 1	gi 50415563 gb BC077583.1	147.2011472
sfrs6	gi 28422194 gb BC044265.1	126.0892513
XIRG protein-like	gi 213623421 gb BC169722.1	87.788455
prickle1	gi 68533725 gb BC098954.1	83.19938866
ZFN384	gi 50415185 gb BC077403.1	69.76482898

<b>Gene</b>	<b>Clone ID</b>	<b>Fold Increase</b>
RAC-beta serine/threonine-protein kinase B	gi 47939912 gb BC072041.1	62.12571541
ccbl-2	gi 30046518 gb BC051239.1	44.93558411
p80 katanin	gi 66910749 gb BC097654.1	40.55422632
zeb2	gi 54648610 gb BC084972.1	33.47771521
Zmiz1	gi 51513014 gb BC080428.1	30.23438945
Angiopoietin 4/5	gi 189442243 gb BC167504.1	27.19110778
HCF-1	gi 52138923 gb BC082658.1	26.78440995
CCR4-NOT transcription complex, subunit 10	gi 50416369 gb BC077237.1	21.48403283
fam107a/b MGC78851	gi 51261937 gb BC079918.1	21.17179772
Nucleoporin Seh1B MGC82845 protein	gi 49118558 gb BC073561.1	19.13482551
PI3K related SMG1 hypothetical protein MGC98890	gi 68226704 gb BC098320.1	17.94963894
Epsin-2 hypothetical protein MGC81482	gi 46249599 gb BC068837.1	16.4173713
srsf7	gi 50603926 gb BC077393.1	16.33581603
sf3b4	gi 28374169 gb BC045264.1	15.37049865
PPTC7 MGC81279 protein	gi 49257211 gb BC071109.1	13.98198898
meis3	gi 54673770 gb BC084920.1	13.07065969
origin recognition complex, subunit 6 homolog-like	gi 50603595 gb BC077746.1	13.01809093
DAXX ? hypothetical protein LOC446279	gi 86577707 gb BC112947.1	12.67764239
ACSL4 hypothetical protein LOC100174803	gi 189442239 gb BC167498.1	11.62060714
Necap2 MGC83534 protein	gi 50927256 gb BC079728.1	10.9853218
Timp3 tissue inhibitor of metalloproteinases-3	gi 38014484 gb BC060423.1	10.67580536
frizzled homolog 7	gi 27503170 gb BC042228.1	9.299494092
Serine/threonine/tyrosine-interacting protein B	gi 54311224 gb BC084791.1	9.188383287
UBADC1 hypothetical protein MGC115132	gi 62471528 gb BC093557.1	8.970846126

<b>Gene</b>	<b>Clone ID</b>	<b>Fold Increase</b>
Cdca A7L transcription factor RAM2	gi 116487713 gb BC126014.1	8.574819986
Klf10 ? hypothetical protein MGC98877	gi 62089536 gb BC092147.1	7.695378855
ivns1abp influenza virus NS1A binding protein	gi 49898869 gb BC076641.1	7.664198955
MGC80567 protein	gi 50417996 gb BC077854.1	7.544735234
LCHN ? hypothetical protein MGC114999	gi 71050977 gb BC098994.1	7.224153034
RABGAP1L hypothetical protein MGC52980	gi 27694685 gb BC043775.1	7.11745345
PTN1 pleiotrophin MGC84465 protein	gi 49257697 gb BC074426.1	6.911246415
arrb1 arrestin, beta 1	gi 49904092 gb BC076815.1	6.832358987
Txnrd3 Thioredoxin reductase 2 MGC81848 protein	gi 51704105 gb BC081053.1	6.824096832
Foxi1 or Foxi4.2a fork head protein	gi 51258369 gb BC080044.1	6.805288292
LIMS1-b LIM domain hypothetical protein MGC81174	gi 47939771 gb BC072204.1	6.795291868
LMO7 LIM domain containing cDNA clone MGC:180040	gi 197245592 gb BC168520.1	6.755182581
arrdc3 arrestin containing hypothetical protein MGC131006	gi 80476391 gb BC108545.1	6.57050044
CANT1 Calcium activated nucleotidase similar to Ca2+-dependent endoplasmic reticulum nucleoside diphosphatase	gi 27370857 gb BC041215.1	6.486609662
D7 protein	gi 58702035 gb BC090198.1	6.413210477
Dact1 dapper 1 Antagonist of beta-catenin FRODO	gi 50418314 gb BC077380.1	6.403341734
RASSF7 Ras assiciation domain containing MGC78972 protein	gi 84105479 gb BC111512.1	6.017970041
Sox11 XLS13B protein	gi 47124741 gb BC070707.1	5.989392572
Myt1 cDNA clone MGC:196991	gi 213626262 gb BC170264.1	5.974437792
zmiz2 MGC86475 protein	gi 51513014 gb BC080428.1	5.658053905
ZC3H7B zinc-finger CCCH-containing 7B MGC80522 protein	gi 50418254 gb BC077837.1	5.638059804
SAP130 HDAC MGC83894 protein	gi 50415582 gb BC077587.1	5.587991945

<u>Gene</u>	<u>Clone ID</u>	<u>Fold Increase</u>
PCNA similar to proliferating cell nuclear antigen	gi 27371152 gb BC041549.1	5.340877685
Stx19 syntaxin 19 hypothetical LOC494752	gi 52354747 gb BC082852.1	5.239206209
HMG-box protein HMG2L1	gi 213625180 gb BC169998.1	5.171640761
Kif20a hypothetical LOC495414	gi 54648449 gb BC084922.1	5.055010856
slc7a3 solute carrier family 7 (cationic amino acid transporter, y <sup>+</sup> system), member 3	gi 27503399 gb BC042222.1	4.989471538
Lmo7 cDNA clone MGC:180040	gi 197245592 gb BC168520.1	4.861028301
Mark2 MAP/microtubule affinity-regulating kinase 2	gi 27694574 gb BC043730.1	4.821716572
Anp32b MGC80871 protein	gi 49118408 gb BC073408.1	4.77985399
cyclin A2	gi 50417439 gb BC077260.1	4.76329664
PPPDE2 peptidase domain containing MGC84710 protein	gi 49256350 gb BC074444.1	4.724302826
CTDP1 FCP1 serine phosphatase	gi 62185666 gb BC092306.1	4.712553945
ornithine decarboxylase-2	gi 28838468 gb BC047954.1	4.690222394
Ube2c hypothetical LOC496302	gi 57032917 gb BC088818.1	4.676640452
Efr3a MGC83628 protein	gi 51950039 gb BC082437.1	4.653269077
Dlg7 discs large hypothetical protein MGC116559	gi 68534624 gb BC099363.1	4.501586994
STXBP3 hypothetical protein MGC115462 syntaxin binding protein 3 (stxbp3)	gi 72679360 gb BC100235.1	4.472242676
Acy-3 aspartoacylase-3	gi 116487526 gb BC125990.1	4.452697089
PTDSS2 cDNA clone MGC:179871	gi 197246680 gb BC168517.1	4.234011971
Tcf-7 transcription factor 7 (T-cell specific, HMG-box)	gi 51261404 gb BC079972.1	4.200569032
Isp1 lymphocyte specific protein 1 hypothetical protein LOC100158340	gi 115528236 gb BC124864.1	4.124150256
NPHP3 nephronophthisis 3 MGC80264 protein	gi 50603779 gb BC077320.1	4.066245125
Med 15 Mediator complex subunit 15 ARC105 protein	gi 47123916 gb BC070536.1	4.029208683

<u>Gene</u>	<u>Clone ID</u>	<u>Fold Increase</u>
cyclin E3	gi 58701930 gb BC090214.1	3.970372822
Fam60a hypothetical protein MGC115222	gi 66910763 gb BC097689.1	3.940864045
AHCTF1 AT hook containing transcription factor 1 MGC83673 protein	gi 49903664 gb BC076775.1	3.892143367
Rhebl1 Ras homolog enriched in brain like 1 hypothetical LOC495056	gi 54037975 gb BC084211.1	3.882231045
RNF8a ring finger protein (C3HC4 type) 8	gi 28279439 gb BC046256.1	3.801782364
CCNT2 cyclin T2 MGC81210 protein	gi 51895950 gb BC081000.1	3.755306852
Tmed2 transmembrane emp24 domain trafficking protein 2 coated vesicle membrane protein, mRNA (cDNA clone MGC:52758 IMAGE:4684109	gi 28277265 gb BC044095.1	3.747391508
Mta1 metastatic associated 1 MGC83916 protein	gi 51950045 gb BC082445.1	3.743645989
MAPK8/Jnk1 mitogen-activated protein kinase 8	gi 28422153 gb BC046834.1	3.733178442
PSMD4 26S proteasome subunit	gi 66910701 gb BC097551.1	3.729782795
Poldip3 polymerase delta interaction protein 3 hypothetical protein MGC114944	gi 62471555 gb BC093543.1	3.720246762
DNAJC5B HSP cDNA clone MGC: 83536	gi 51703523 gb BC081115.1	3.720172358
NCBP2 Nuclear cap binding protein 2	gi 49117074 gb BC072902.1	3.701358817
FXDY FXDY domain containing ion transport	gi 125859119 gb BC129686.1	3.694185141
Ano5 Anoctamin 5 or Tmem16e	gi 50418049 gb BC077486.1	3.642280513
Not Annotated	gi 62739385 gb BC094151.1	3.628720112
Ttc30a tetratricopeptide repeat domain 30a	gi 47938700 gb BC072174.1	3.547737229
F2rl1 Coagulation factor 2 receptor like 1	gi 57033014 gb BC088935.1	3.518659172
CSDA cols shock protein domain containing A	gi 161611734 gb BC155913.1	3.51654861
FUS Fused in Sarcoma?	gi 49522197 gb BC074437.1	3.505453855
Exo1 exonuclease 1	gi 54035217 gb BC084102.1	3.494289274
Cfp complement factor properdin	gi 50415018 gb BC077925.1	3.468804465

<b>Gene</b>	<b>Clone ID</b>	<b>Fold Increase</b>
Ferritin light chain	gi 34785676 gb BC057216.1	3.464575104
cdc25c	gi 213626377 gb BC169346.1	3.456754005
SLC44a1 solute carrier family 44 member 1	gi 52354612 gb BC082837.1	3.306234736
PCF11 cleavage and poly-adenylation factor	gi 50414592 gb BC077233.1	3.277333059
Slc9a1 or NHE3 solute carrier family 9 member 3	gi 157422994 gb BC153791.1	3.274941479
Anks1a Ankyrin repeat and sterile alpha motif domain containing 1a	gi 47682305 gb BC070831.1	3.249886264
ap2b1 adaptor-related protein complex 1 beta 1 subunit	gi 120538239 gb BC129531.1	3.240669681
Not Annotated	gi 76780224 gb BC106027.1	3.21623043
Ctnnd1 Catenin (Cadherin associated protein) delta-1	gi 213623207 gb BC169434.1	3.210767484
GCAT Glycine C-acetyltransferase	gi 28704125 gb BC047258.1	3.210735376
beta arrestin	gi 49256118 gb BC072973.1	3.173896459
slc9a3r2	gi 55778573 gb BC086464.1	3.167840103
CTDP1 (carboxy-terminal domain, RNA polymerase II, polypeptide A) phosphatase, subunit 1	gi 51950263 gb BC082378.1	3.162965383
MAX bHLH	gi 47123961 gb BC070710.1	3.144295944
MPV17l	gi 51261416 gb BC079982.1	3.11285403
Fibronectin 1	gi 49114986 gb BC072841.1	3.110364743
Splicing factor (sfrs5)	gi 47717980 gb BC070967.1	3.1059201
transmembrane protein 45B	gi 120538262 gb BC129609.1	3.030355684
lysine (K)-specific demethylase 6A (kdm6a)	gi 50603932 gb BC077424.1	3.026903047
RalGDS/AF-6	gi 84105479 gb BC111512.1	2.963378492
Mek-2	gi 27694983 gb BC043913.1	2.955122189
calpain 2, (m/II) large subunit (capn2)	gi 39645066 gb BC063733.1	2.924548179
PHD finger protein 12 (phf12)	gi 46249573 gb BC068803.1	2.89562217
pax interacting (with transcription-activation domain) protein 1 (paxip1)	gi 50417566 gb BC077588.1	2.822971349

<u>Gene</u>	<u>Clone ID</u>	<u>Fold Increase</u>
mediator complex subunit 16 (med16)	gi 62471580 gb BC093546.1	2.822152806
xRMD-2 microtubule-associated protein tyrosine kinase 2 (tyk2)	gi 58702063 gb BC090235.1	2.803700074
methyltransferase like 3 (mettl3)	gi 49118136 gb BC073112.1	2.790804764
glycine amidinotransferase (L-arginine:glycine amidinotransferase) (gatm)	gi 46249483 gb BC068672.1	2.782222309
syntaxin 5 (stx5)	gi 28838491 gb BC047973.1	2.746369891
inhibitor of kappa light polypeptide gene enhancer in B-cells, kinase beta (ikbkb)	gi 76779222 gb BC106704.1	2.704962367
G-2 and S-phase expressed 1 (gtse1)	gi 47939754 gb BC072192.1	2.686442963
RBL1	gi 62471553 gb BC093540.1	2.683239948
nucleoporin 93kDa (nup93)	gi 47123210 gb BC070856.1	2.680418663
embryonic ectoderm development (eed)	gi 27924241 gb BC045089.1	2.672333338
ring finger and CCCH-type domains 1 (rc3h1)	gi 50603665 gb BC077425.1	2.655016847
integrin, beta 5	gi 46250191 gb BC068669.1	2.646867856
ataxin 2 (atxn2)	gi 49899756 gb BC076844.1	2.636182901
chromosome 19 open reading frame 2 (c19orf2)	gi 66910767 gb BC097692.1	2.634583223
PRP4 pre-mRNA processing factor 4 homolog (prpf4)	gi 50415135 gb BC077366.1	2.630865817
protein phosphatase methylesterase 1 (ppme1)	gi 51703477 gb BC081044.1	2.62131998
orthodenticle homeobox 2 (otx2-a)	gi 50418398 gb BC077600.1	2.617432826
chromosome 13 open reading frame 34 (c13orf34)	gi 50417481 gb BC077357.1	2.616883223
DAZAP1	gi 49523107 gb BC075159.1	2.599294339
FSHD region gene 1 (frg1)	gi 50604139 gb BC077252.1	2.585999275
serine/threonine kinase 11 interacting protein (stk11ip)	gi 49256477 gb BC074376.1	2.555875944
carboxy-terminal kinesin 2	gi 47682952 gb BC070809.1	2.553165597
survival of motor neuron 2, centromeric (smn2)	gi 54038135 gb BC084431.1	2.538623487
	gi 46249513 gb BC068721.1	2.535840144

<b>Gene</b>	<b>Clone ID</b>	<b>Fold Increase</b>
sall1 (Sal-like 1)	gi 37590272 gb BC059284.1	2.505331347
NIMA (never in mitosis gene a)-related kinase 2 (nek2)	gi 27696903 gb BC043822.1	2.503175185
ZF-containing (posterior protein)	gi 213623475 gb BC169799.1	2.493496644
drebrin-like (dbnl)	gi 49257631 gb BC074277.1	2.479066307
jumonji domain containing 6 (jmjd6-b)	gi 28277358 gb BC045252.1	2.4687995
inhibitor of DNA binding 3, dominant negative helix-loop-helix protein (id3-a)	gi 27696824 gb BC044039.1	2.448101925
chaperonin containing TCP1, subunit 8 (theta) (cct8)	gi 67678231 gb BC097574.1	2.447348026
LIM domain containing preferred translocation partner in lipoma (lpp)	gi 62740239 gb BC094110.1	2.445439839
cytochrome c-1 (cyc1)	gi 71052231 gb BC099350.1	2.442233526
KIAA0182 (kiaa0182)	gi 120537359 gb BC129052.1	2.438699731
5-aminoimidazole-4-carboxamide ribonucleotide formyltransferase/IMP cyclohydrolase (atic)	gi 76779775 gb BC106381.1	2.42732299
ribonucleoprotein A1a (hnrnpa1)	gi 47938743 gb BC072090.1	2.419006697
caspase 3, apoptosis-related cysteine peptidase casp3	gi 68533747 gb BC098991.1	2.408087828
ubiquitin-conjugating enzyme E2G 1 (UBC7 homolog) (ube2g1)	gi 28839012 gb BC047985.1	2.407955386
drebrin-like (dbnl)	gi 49257631 gb BC074277.1	2.388809202
PTK7 protein tyrosine kinase 7 (ptk7)	gi 148922111 gb BC146640.1	2.387741643
integrator complex subunit 2 (ints2)	gi 47125091 gb BC070524.1	2.387717766
PRP4 pre-mRNA processing factor 4 homolog B (prpf4b)	gi 125858002 gb BC129065.1	2.375801846
Transmembrane protein 33 (tmem33)	gi 49903380 gb BC076764.1	2.371301594
non-SMC condensin II complex, subunit D3 (ncapd3)	gi 49116983 gb BC073714.1	2.363179599
SIN3 homolog B, transcription regulator (sin3b)	gi 120538596 gb BC129063.1	2.353559822
splicing factor, arginine/serine-rich 18 (sfrs18)	gi 47940261 gb BC072160.1	2.350873591
mediator complex subunit 23 (med23)	gi 39645714 gb BC063725.1	2.349851184

<b>Gene</b>	<b>Clone ID</b>	<b>Fold Increase</b>
phospholipase A2-activating protein (plaa)	gi 115528262 gb BC124847.1	2.344309729
minichromosome maintenance complex component 4 (mcm4-b)	gi 49115033 gb BC072870.1	2.342847336
NOP2/Sun domain family, member 2 (nsun2)	gi 66912075 gb BC097814.1	2.339817652
general transcription factor IIE, polypeptide 2, beta 34kDa (gtf2e2)	gi 58403335 gb BC089287.1	2.320004209
Rho GTPase activating protein 19 (arhgap19)	gi 48734660 gb BC072338.1	2.309370554
CCR4-NOT transcription complex, subunit 10 (cnot10-b)	gi 46250097 gb BC068748.1	2.298100702
lysine (K)-specific demethylase 3A (kdm3a-a)	gi 47506877 gb BC070982.1	2.296984096
zinc finger and BTB domain containing 44 (zbtb44)	gi 47124748 gb BC070714.1	2.293259115
phosphatidylinositol glycan anchor biosynthesis, class T (pigt)	gi 52354598 gb BC082818.1	2.284755462
heterogeneous nuclear ribonucleoprotein A3 (hnrrnpa3)	gi 213625122 gb BC169881.1	2.283526595
Putative ortholog of von Hippel-Lindau binding protein 1 (Prefoldin subunit 3)	gi 163916339 gb BC157499.1	2.278221284
nucleoporin 37kDa (nup37)	gi 51703531 gb BC081128.1	2.271537693
activating transcription factor 1 (ATF1)	gi 61403334 gb BC092037.1	2.266325959
Nedd4 family interacting protein 2 (ndfip2)	gi 50924805 gb BC079714.1	2.262854343
	gi 33416619 gb BC055957.1	2.260893298
proteasome (prosome, macropain) 26S subunit, ATPase, 3 (psmc3)	gi 28422358 gb BC046948.1	2.253753391
family with sequence similarity 109, member B (fam109b)	gi 47122977 gb BC070645.1	2.237428018
translation initiation factor 4E family member 3 (eif4e3-a)	gi 49257962 gb BC071126.1	2.230893103
ets variant gene 4	gi 50417509 gb BC077414.1	2.224884491
G kinase anchoring protein 1 (gkap1-a)	gi 49118875 gb BC073450.1	2.208726268
zinc finger transcription factor SALL4	gi 52138969 gb BC082637.1	2.190818022

<u>Gene</u>	<u>Clone ID</u>	<u>Fold Increase</u>
chromobox homolog 5 (cbx5)	gi 32766466 gb BC054962.1	2.18484743
CCR4-NOT transcription complex, subunit 6-like (cnot6l-a)	gi 47506927 gb BC071015.1	2.17052701
uridine-cytidine kinase 2 (uck2)	gi 52354745 gb BC082833.1	2.153018907
YY1 transcription factor (yy1-b)	gi 50925274 gb BC079731.1	2.144522678
karyopherin alpha 4 (importin alpha 3) (kpna4)	gi 47122818 gb BC070533.1	2.143067042
syntaxin 5 (stx5)	gi 76779222 gb BC106704.1	2.132374185
PRP4 pre-mRNA processing factor 4 homolog B (prpf4b)	gi 54038077 gb BC084355.1	2.120332678
oxoglutarate (alpha-ketoglutarate) dehydrogenase (lipoamide) (ogdh)	gi 49118216 gb BC073213.1	2.110063412
acidic (leucine-rich) nuclear phosphoprotein 32 family, member B (anp32b)	gi 27503409 gb BC042250.1	2.104752746
AT hook containing transcription factor 1 (ahctf1)	gi 55250536 gb BC086281.1	2.095665156
proline-rich nuclear receptor coactivator 2 (pnrc2-b)	gi 54038003 gb BC084247.1	2.080782448
YY1 transcription factor	gi 50415555 gb BC077581.1	2.079401267
Ptk7	gi 38014809 gb BC060500.1	2.074966481
H3 histone, family 3B (H3.3B) (h3f3b)	gi 47506868 gb BC070966.1	2.05094159
bromodomain containing 1 (brd1)	gi 49118425 gb BC073421.1	2.046475407
mllt6	gi 52354628 gb BC082872.1	2.041361526
RAS oncogene family (rab18)	gi 33416685 gb BC056054.1	2.03028667
RAB6A, member RAS oncogene family (rab6a)	gi 28302337 gb BC046683.1	2.027277987
transcription factor 3 (E2A immunoglobulin enhancer binding factors E12/E47) (tcf3)	gi 28422165 gb BC046840.1	2.026584776
cell division cycle 20 homolog (cdc20)	gi 50370183 gb BC076805.1	2.012178568
sema domain, transmembrane domain (TM), and cytoplasmic domain, (semaphorin) 6D (sema6d)	gi 213626595 gb BC169687.1	2.010828849
lethal giant larvae homolog 1 (llgl1)	gi 47123133 gb BC070788.1	2.000831812